

DISSERTATION

MOLECULAR CHARACTERIZATION OF THE PROTEIN-PROTEIN
INTERACTION BETWEEN HTLV-1 TAX AND GSK-3 β

Submitted by

Guoliang Wang

Department of Biochemistry and Molecular Biology

In partial fulfillment of the requirements

For the Degree of Doctor of Philosophy

Colorado State University

Fort Collins, Colorado

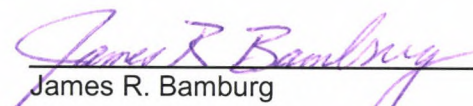
Spring 2010

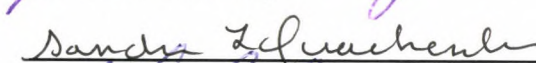
COLORADO STATE UNIVERSITY


December 10th, 2009

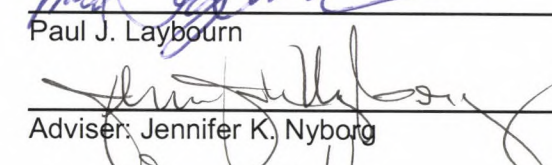
WE HEREBY RECOMMEND THAT THE DISSERTATION PREPARED
UNDER OUR SUPERVISION BY GUOLIANG WANG ENTITLED *MOLECULAR
CHARACTERIZATION OF THE PROTEIN-PROTEIN INTERACTION BETWEEN
HTLV-1 TAX AND GSK-3 β* BE ACCEPTED AS FULFILLING IN PART THE
REQUIREMENTS FOR THE DEGREE OF DOCTOR OF PHILOSOPHY.

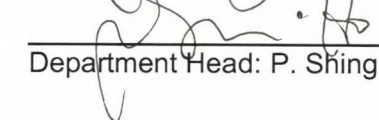
Committee on Graduate Work


James R. Bamberg


Sandra L. Quackenbush


Paul J. Laybourn


Adviser: Jennifer K. Nyborg


Department Head: P. Shing Ho

ABSTRACT OF DISSERTATION

MOLECULAR CHARACTERIZATION OF THE PROTEIN-PROTEIN INTERACTION BETWEEN HTLV-1 TAX AND GSK-3 β

The human T-cell leukemia virus type 1 (HTLV-1) encodes a viral oncoprotein termed Tax, which plays a major role in transforming HTLV-1-infected cells. Tax is a potent transcriptional activator that stimulates HTLV-1 viral and cellular gene transcription. In addition, Tax disrupts a number of cell signaling pathways involved in cell growth and survival. Glycogen synthase kinase-3 β (GSK-3 β) is a ubiquitously expressed serine/threonine kinase present in all eukaryotic cells, which functions as a critical regulator of a wide range of cell signaling pathways. As GSK-3 β is constitutively active in resting cells, it is primarily regulated through inhibition. Ser-9 phosphorylation is inhibitory to the kinase activity of GSK-3 β . Deregulation of GSK-3 β has been linked to many human diseases such as Alzheimer's disease and cancers.

It has been reported in Aida Ulloa's thesis that Tax inhibits GSK-3 β kinase activity toward both primed and non-primed substrates through direct association. To delineate the protein-protein interaction between Tax and GSK-3 β , we compared the amino acid sequence of Tax with a well-characterized short peptide deriving from the GSK-3 β interacting domain (GID) of Axin, and found that Tax contains a notable amino acid sequence homology to Axin GID. The region spanning Tax amino acids 185 – 205 has 24% sequence identity and 19% similarity with Axin GID. We named this region the putative Tax GID. We characterized the putative Tax GID biochemically, and discovered that a longer

peptide (Tax aa. 138 – 205) of the putative Tax GID strongly inhibits GSK-3 β kinase activity *in vitro*. Bioinformatics computation was used to predict the secondary structure of the Tax GID, which was further used in our docking test to identify a potential binding interface in GSK-3 β . This was tested by GST pull-down and Co-IP assays using point and deletion mutants. In addition, the effects of Tax-GSK-3 β interaction on the downstream β -catenin and NFAT pathways were characterized by luciferase reporter assays. However, unexpectedly, we observed that Tax expression has little effects on β -catenin and NFAT transcriptional activation.

Guoliang Wang
Department of Biochemistry and Molecular Biology
Colorado State University
Fort Collins, Colorado 80523
Spring 2010

ACKNOWLEDGEMENTS

I am glad that I spent the last five years at Colorado State University to pursue a PhD in Biochemistry. I have received enormous amount of help from many people that I always appreciate. First of all, I would like to express my deepest gratitude to my mentor, Dr. Jennifer Nyborg, for her mentorship, inspiration, encouragement, and support during my study in her laboratory. Her passion and high standards in science helped tremendously to shape me as a scientist. I have also learned great scientific and work ethics from her to do good science. I would also like to give my heartfelt thanks to my committee members for working with me during my graduate study. I am grateful to the past and current members of the Nyborg laboratory who are helpful. They made my study and the learning process enjoyable in the laboratory. I appreciate Holli Giebler and Dr. Youngmi Kim for their advice and help with my project and thesis writing. I also appreciate Dinaida Egan and Jeanne Mick for training me to purify protein using chromatography and other techniques.

Last but not least, I would like to thank my entire family for their support and love. Without my parents' encouragement, I would not have decided to go this far in my education. I appreciate my wife for taking care of me during my study at CSU. Our lovely baby girl Marina Summer Wang was born on August 22, 2009, and she brings us enormous happy moments.

TABLE OF CONTENTS

TITLE PAGE.....	I
SIGNATURE PAGE.....	II
ABSTRACT OF DISSERTATION.....	III
ACKNOWLEDGEMENTS	V
TABLE OF CONTENTS	VI
 CHAPTER 1 INTRODUCTION TO HTLV-1, TAX, AND GSK-3B	 1
1.1 HUMAN T-CELL LEUKEMIA VIRUS TYPE 1 (HTLV-1)	1
1.1a Adult T-cell Leukemia	2
1.1b HTLV-1 Life Cycle.....	3
1.1c HTLV-1 Genome	6
1.2 THE HTLV-1 TAX PROTEIN	8
1.2a Regulation of Viral Gene Expression by Tax	8
1.2b Tax Deregulation of Cell Signaling Pathways and Gene Expression...	9
1.2c Functional Regions of Tax	11
1.2d Major Tax Interactome	14
1.3 THE MULTI-TASKING KINASE: GSK-3	16
1.3a The Structure of GSK-3 β	17
1.3b Regulation of GSK-3 β	18
1.3c Wnt Signaling.....	20
1.3d Cellular Targets of GSK-3 β	22
1.3e Cellular Proteins Interacting with GSK-3 β	26
1.4 THESIS RESEARCH OBJECTIVES AND SIGNIFICANCE	29
 CHAPTER 2 MOLECULAR CHARACTERIZATION OF GSK-3B	
INACTIVATION BY HTLV-1 TAX.....	32
2.1 ABSTRACT	32
2.2 INTRODUCTION	34
2.3 RESULTS	37
2.3a Tax inhibits GSK-3 β via direct interaction.	37
2.3b Identification of GSK-3 β interacting domain in Tax.	39
2.3c Tax GID inhibits GSK-3 β	44

2.3d Bioinformatics predictions and experimental analysis of the Tax-GSK-3 β interaction.	52
2.4 DISCUSSION.....	60
2.5 ACKNOWLEDGEMENTS	63
CHAPTER 3 SUPPLEMENTAL DATA	64
3.1 THE TAX 3A MUTANT (E193A, L194A, AND L195A) SHOWS WEAKER INTERACTION WITH GSK-3B.....	64
3.2 TAX 5A MUTANT IS DEFECTIVE FOR QUATERNARY COMPLEX FORMATION WITH CREB/VCRE/KIX.	66
3.3 TAX 5A MUTANT INHIBITS GSK-3B.	68
3.4 TAX IS PHOSPHORYLATED BY GSK-3B IN VITRO.	69
3.5 TAX HAS LITTLE EFFECT ON B-CATENIN/TCF-4 TRANSCRIPTIONAL ACTIVATION.	71
3.6 TAX HAS NO EFFECT ON NFAT TRANSCRIPTIONAL ACTIVATION.	75
CHAPTER 4 MATERIALS AND METHODS	78
4.1 CLONING, EXPRESSION, AND PURIFICATION OF RECOMBINANT PROTEINS.	78
4.2 GST PULL-DOWN ASSAYS.	80
4.3 MAMMALIAN EXPRESSION PLASMIDS, CELL CULTURE AND TRANSIENT TRANSFECTION ASSAYS.	80
4.4 ANTIBODIES.	81
4.5 IN VITRO GSK-3B KINASE ASSAYS.....	81
4.6 PHOSPHATASE ASSAYS.	82
4.7 CO-IMMUNOPRECIPITATION ASSAYS.	82
4.8 ELECTROPHORETIC MOBILITY SHIFT ASSAYS (EMSAs).....	83
4.9 LUCIFERASE REPORTER ASSAYS.	83

CHAPTER 5 FUTURE DIRECTIONS	85
REFERENCES	90

Chapter 1 Introduction to HTLV-1, Tax, and GSK-3 β

Chapter 1 covers the background and significance of human T-cell leukemia virus type 1 (HTLV-1) and the two well-known diseases it causes: adult T-cell leukemia (ATL) and tropical spastic paraparesis. Selected details of the viral RNA genome, life cycle and the cell signaling pathways affected by Tax are also included to give readers a broader picture of the retrovirus. This will be followed by an introduction to the two major protein players in this study: Tax and GSK-3 β . The last part of this chapter presents the rationale, objectives and significance of the study.

1.1 Human T-cell Leukemia Virus Type 1 (HTLV-1)

Clustered cases of adult T-cell leukemia (ATL) in West part of Japan were a key event for the discovery of the first human retrovirus, HTLV-1, in the late 1970's. That evoked enormous attention from physicians, oncologists, and virologists. Scientists from Japan and the United States separately identified HTLV-1 as the etiological agent responsible for ATL in the early 1980's. The symptoms of ATL include hypercalcemia, lytic bone lesions and skin lesions. ATL cells have remarkable lobulated nuclei, chromosomal abnormalities, and surface phenotypes (1, 2). In addition to ATL, researchers found the association between HTLV-1 and another disease known as tropical spastic paraparesis/HTLV-1 associated myelopathy (TSP/HAM), which is immune-mediated.

HTLV-1 is primarily transmitted vertically from mother to infant through breastfeeding or *in utero*. Additionally, HTLV-1 can be transmitted horizontally via blood transfusion or sexual intercourse. The transmission of HTLV-1 virions rely on cell-to-cell contact within infected individuals, as there is no detectable virions in the serum. Most infected individuals remain asymptomatic throughout their lifetime, only a small percentage (< 5%) of the infected population develops HTLV-1-associated diseases such as ATL. An average latency period of 20 – 30 years has been reported between the time of HTLV-1 infection and development of disease (3). Currently, there are approximately 10 – 20 million people infected by HTLV-1 in the world (4).

1.1a Adult T-cell Leukemia

ATL is a highly aggressive malignancy of CD4⁺ T-lymphocytes, which is almost always fatal. It is characterized by rapid and uncontrolled proliferation of mature transformed CD4⁺ and CD25⁺ T-cells. The mean survival of patients in the acute phase of ATL is only 6 months. The symptoms of ATL include hypercalcemia, lytic bone lesions, and skin lesions due to infiltrating leukemic cells.

In HTLV-1 infected individuals, the provirus is randomly integrated in the chromosomal DNA of the host's T-cells. However, in ATL patients, the HTLV-1 provirus is integrated in a clonal fashion, with one copy of the provirus integrated in the same chromosomal locus in each cell. Tumor cells derived from ATL patients do not have detectable replicating virus, suggesting that HTLV-1 is not actively involved in maintaining the leukemic state, but rather, is involved in

promoting cellular transformation. The spread of HTLV-1 within infected individuals depends on the mitotic replication of T-cells.

The pathogenesis of ATL appears to involve a process of viral protein expression leading to oncogenic mutation and cellular immortalization. Furthermore, HTLV-1 has evolved complex apoptosis evasion strategies, and HTLV-1-infected cells are highly resistant to multiple pro-apoptotic stimuli, including death receptor-mediated stimuli, DNA damage-induced stimuli, and γ -irradiation compared to uninfected normal cells (5-9).

1.1b HTLV-1 Life Cycle

The HTLV-1 virion is about 100 nm in diameter, and has an envelope at the outside, decorated with transmembrane glycoproteins. The internal nucleocapsid is a roughly spherical, which contains two identical single-stranded, positive-sense genomic RNAs. Moreover, the catalytically active enzymes integrase, protease and reverse transcriptase reside in the nucleocapsid.

The HTLV-1 life cycle begins with the attachment of virions to receptors on the surface of host cells, followed by injection of the virion core content into the host cell cytoplasm. HTLV-1 can infect a variety of cell types, including T-lymphocytes, B-lymphocytes, monocytes, and fibroblast (8). Glucose transporter 1 (GLUT-1) has been identified as receptor for HTLV-1, which is ubiquitously expressed on cell surfaces (9).

HTLV-1 utilizes its reverse transcriptase to synthesize proviral double-stranded DNA from the single-stranded RNA genome, which is then integrated

into the host cell genome with the aid of the viral integrase. After the chromosomal integration, the HTLV-1 provirus replicates during host cellular DNA replication (Fig. 1.1). The viral genome integration is essential for lifelong infection and evasion of host immune clearance, allowing diseases with long latency.

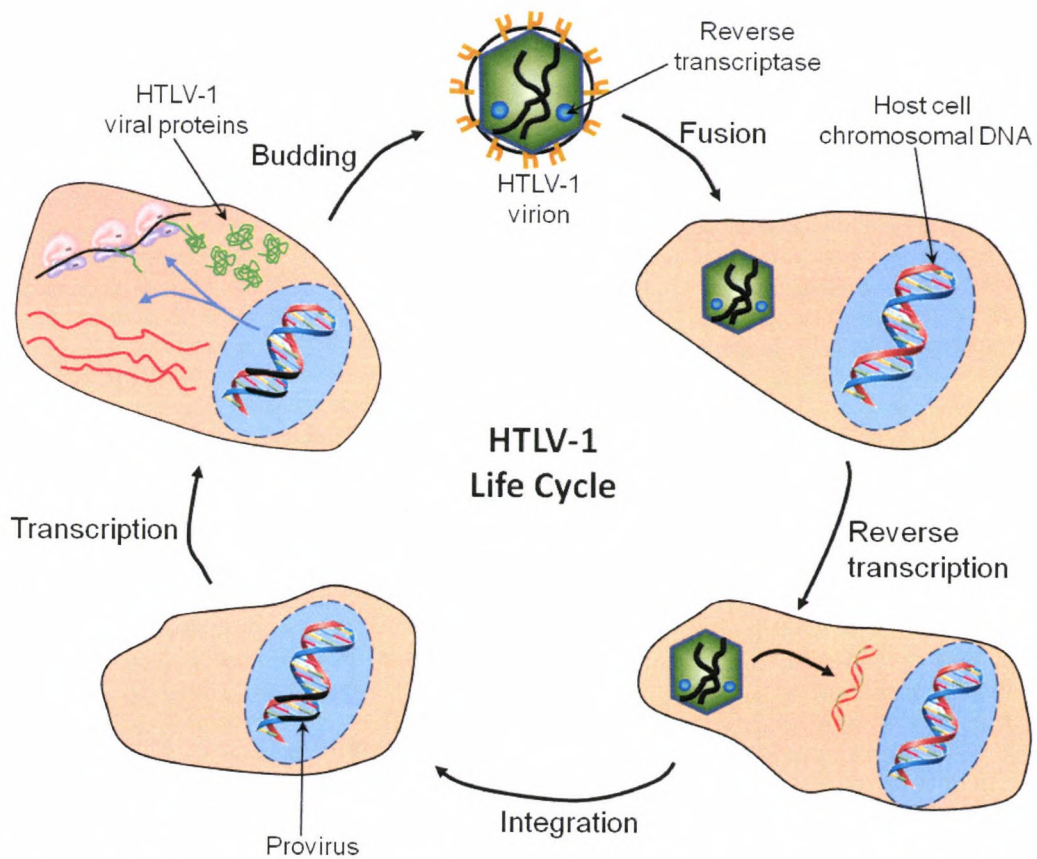


Figure 1.1. The HTLV-1 life cycle. Major events in the viral replication cycle include adsorption and entry, reverse transcription, nuclear transport and integration, viral gene expression, viral protein synthesis, processing, and assembly.

1.1c HTLV-1 Genome

HTLV-1 belongs to the δ -type retrovirus genus, which also includes bovine leukemia virus (BLV), HTLV-2, and simian T-cell leukemia virus (STLV). The HTLV-1 proviral genome is about 9 kb, and contains *gag*, *pro*, *pol* and *env* genes, flanked by long terminal repeats (LTR). The HTLV-1 LTR contains the viral promoter and other regulatory elements and is divided into the U3, R, and U5 regions. The *gag* region encodes the capsid (CA), nucleocapsid (NC), and matrix (MA) retroviral structural proteins. The *env* gene encodes the transmembrane (TM/gp 21) and surface (SU/gp 46) glycoproteins, whereas the *pol* gene encodes reverse transcriptase (RT), integrase (IN), and protease, the latter of which cleaves viral polyproteins. A schematic of the HTLV-1 genome and provirus is shown in figure 1.2. The U3 region contains three highly conserved 21-base-pair (bp) repeat sequences called viral cyclic AMP response elements (vCREs) that control proviral transcription (10). The HTLV-BLV groups of retroviruses share a pX region located between *env* open reading frame (ORF) and the 3' LTR. The pX region encodes a few major nonstructural proteins including Tax, Rex, and accessory proteins (p12, p30, p21 and HBZ). The molecular weights of Tax and Rex are 40 kDa and 27 kDa, respectively. Tax protein is critical for viral gene transcriptional activation. It is also responsible for promoting cellular proliferation, which is believed to contribute to ATL. Rex is a post-transcriptional regulatory protein. Increased expression of Rex suppresses the expression of the fully spliced pX mRNA.

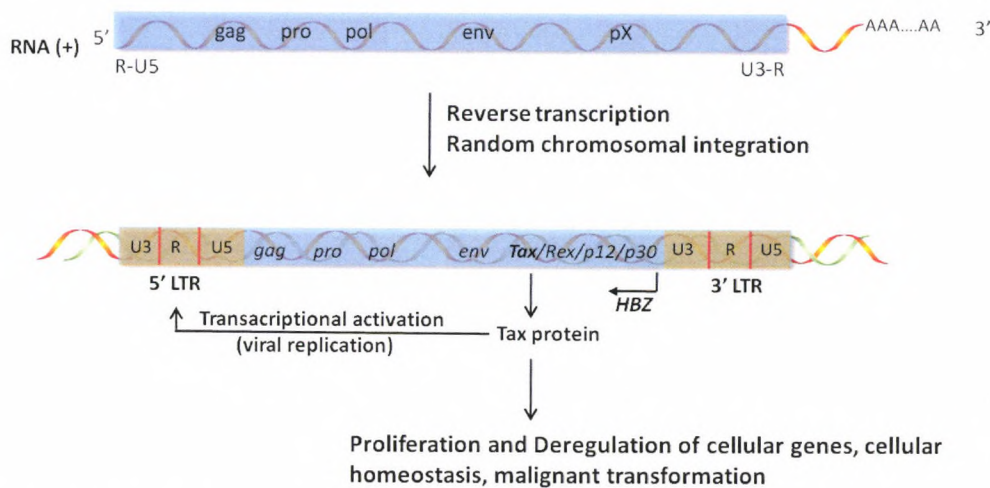


Figure 1.2. Schematic representation of the HTLV-1 RNA viral genome and proviral genome. The gag and pol proteins are expressed from the full-length genomic viral transcript, which encodes the transmembrane glycoproteins and protease. The env protein, a component of the envelope, is translated from a singly-spliced viral RNA. The Tax and Rex proteins are expressed from a doubly spliced viral RNA. Tax is a potent viral transcriptional activator that binds the promoter region of HTLV-1 genome and deregulates cellular genes.

1.2 The HTLV-1 Tax Protein

The 40-kD Tax protein is essential for viral replication and malignant transformation of HTLV-1-infected T-cells (11). Tax also functions as a potent transcription activator of viral and cellular genes, and has been reported to disrupt a number of cell signaling pathways by deregulating the expression or function of key protein regulators in important cell signaling pathways (11, 12).

1.2a Regulation of Viral Gene Expression by Tax

Tax expression is necessary for efficient production of the viral mRNA (13-16). Tax activates HTLV-1 gene expression via interactions with the activating transcription factors, cyclic AMP response element binding protein (ATF/CREB) family members and the paralogous coactivators CREB-binding protein (CBP) and p300, which assemble into a multiprotein complex on the 21-bp enhancer elements known as viral CREs (vCREs). There are three vCREs upstream of the RNA transcription initiation site in HTLV-1 LTR. Each enhancer element carries a core off-consensus CRE immediately flanked by GC-rich DNA sequences, which is conserved in all HTLV family members. The cellular transcription factor CREB binds the vCRE as a homodimer through its leucine zipper domain, and Tax associates with the vCREs through protein-DNA interactions and protein-protein interactions with CREB (17, 18). The three vCREs of HTLV-1 serve as *cis*-acting enhancer elements, which are required for Tax transactivation (10, 19-23).

Kwok et al (24) found that Tax and CREB activate HTLV-1 transcription through recruitment of the transcriptional co-activator CBP to the promoter. Furthermore, they showed that the vCRE activation is independent of CREB

phosphorylation (24). In sharp contrast, however, a recent study from the Nyborg laboratory indicated that the Tax and CREB complex on vCRE is deficient for full-length CBP/p300 recruitment and transcriptional activation (25). Tax requires association with phosphorylated CREB for recruitment of CBP/p300. Tax, present at the GC-rich sequences flanking the vCREs region (17), binds pCREB and stabilizes the protein complex, which therefore facilitates the recruitment of CBP/p300 to vCREs and the subsequent transcriptional activation (26). The transcriptional activity of CREB is largely activated by phosphorylation of its Ser-133 residue, which is mediated by numerous protein kinases (27-33). Elevated levels of phosphorylated CREB have been reported in several HTLV-1-infected T-cell lines (26). Furthermore, several studies show that Tax induces CREB phosphorylation *in vivo* (26, 34, 35), driving constitutive elevated viral and cellular gene expression.

1.2b Tax Deregulation of Cell Signaling Pathways and Gene Expression

Tax has been reported to immortalize primary rodent cells and primary human T-cells derived from peripheral blood or cord blood (11, 36, 37). In addition to the fact that Tax is a potent transcriptional activator of HTLV-1 gene expression, Tax is involved in deregulating numerous cell signaling pathways, leading to alteration of gene expression patterns, cellular proliferation, malignant transformation, and tumorigenesis. Tax stimulates transcription of numerous cellular genes through deregulating signal transduction pathways including the phosphoinositide 3-kinase (PI3K), NFAT, NF- κ B and AP-1 pathways. Comparison of gene expression profiles between HTLV-infected and uninfected

T-cells revealed numerous differences in the expression of signaling molecules including cytokine receptors and cytokines (38, 39). These alterations caused by Tax contribute to cellular transformation.

The PI3K/Akt signaling pathway plays an important role in regulating cell cycle progression and cell survival. Activation of the PI3K/Akt signaling pathway is associated with cellular growth stimulation and the evasion of apoptosis. PI3K is a heterodimer enzyme composed of a p85 regulatory subunit and a p110 catalytic subunit (40) that phosphorylates phosphoinositides and leads to the phosphorylation and activation of Akt (aka. Protein Kinase B). PI3K/Akt is constitutively activated in HTLV-transformed Rat-1 cells and is involved in cell transformation (41). Moreover, Akt is a serine/threonine kinase whose activation is oncogenic and is found in many types of cancer (42).

The activity of PI3K is tightly regulated in normal cells by many different mechanisms. It is currently believed that the p110 and p85 subunits form a complex in the cytoplasm of resting cells; the p85 regulatory subunit not only stabilizes the p110 catalytic subunit but also inhibits its lipid kinase activity (43, 44). Peloponese and Jeang (42) utilized Co-IP studies to demonstrate that Tax binds the p85 but not the p110 subunit, which diminishes the interaction between p110 and p85 in Tax-expressing T-cell lines. This gives rise to constitutive activation of PI3K in Tax-expressing cells.

Recent studies indicated that Tax dysregulates the β -catenin pathway through activating the PI3K/Akt pathway, which results in the stabilization and accumulation of β -catenin in cytoplasm (45, 46). Stabilized β -catenin co-activates

the human T-cell factor (Tcf)/lymphoid enhancer factor (Lef) target genes that include well-known oncogenes such as c-myc (47) and cyclin D1 (48). Aberrant stabilization of β -catenin is highly oncogenic and high-level expression of β -catenin is found in several leukemic cell lines (49-51) .

1.2c Functional Regions of Tax

The full-length HTLV-1 Tax protein consists of 353 amino acids that can be divided into multiple functional regions (Fig. 1.3). Tax interacts with a variety of host transcriptional factors and modulates their functions directly or indirectly. Tax functionality relies heavily on its subcellular localization in the nucleus where it interacts with and modulates nuclear transcription factors. The nuclear localization signal (NLS) of Tax is located in the amino terminal 58 residues (52, 53) and consists of a weakly basic domain with a large number of cysteine and histidine residues. The N-terminal 58-amino acid cysteine/histidine rich region makes up a zinc-finger-like motif within Tax that is important for the HTLV-1 LTR transactivation function and for correct protein folding (54). In addition, the Tax NLS region is involved in interaction with CREB (55, 56).

Tax dimerization is required for optimal transactivation of gene transcription (57), as indicated by yeast two-hybrid assays and mutational analysis (58). The dimerization region of Tax includes amino acids 127 – 228. Tax dimerization increases its activity and therefore is important for transcriptional activation of the HTLV-1 promoter; point mutants in this domain are unable to mediate viral transcription *in vivo* (57, 59, 60).

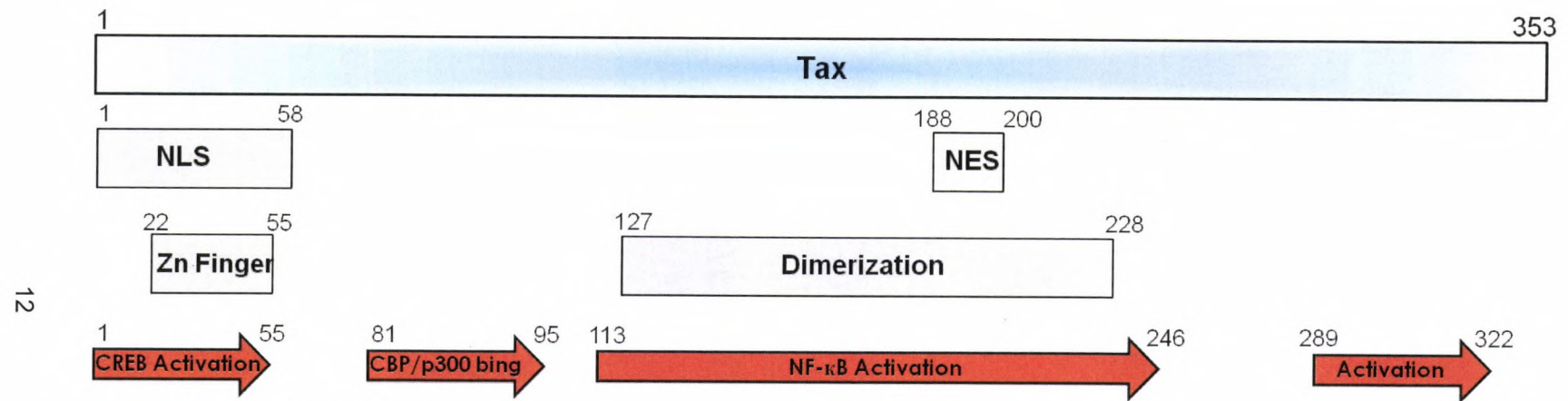


Figure 1.3. Functional Regions of HTLV-1 Tax.

NLS: nuclear localization signal; **NES:** nuclear export signal. Adapted from reference (68).

Seminal work by Lenzmeier et al provided the first evidence that Tax directly binds to the minor groove of the GC-rich sequences of the viral CREs (17, 61). Interruption of the Tax protein-DNA interaction abolishes Tax transactivation activity *in vitro*, therefore the protein-DNA interaction is critical for Tax to transactivate gene expression (62). The DNA interaction region in Tax was isolated between amino acids 89 and 110 (61).

Mutational analysis of the full-length Tax uncovered a minimal transactivation domain in the carboxyl terminus spanning amino acids 284–325 (63). The minimal transactivation is thought to be responsible for forming important protein-protein interactions with basal transcription factors and/or coactivators (64-66). The M47 Tax mutant, a double-point mutation of amino acids 319 and 320 (L319R/L320S) in the transactivation domain, abrogates HTLV-1 transcription *in vivo*. Another study using the M47 Tax mutant suggested that the Tax transactivation domain plays a role in recruiting RNA polymerase II transcriptional machinery and/or coactivators (64).

As noted earlier, Tax plays an important role recruiting the transcription coactivators CBP/p300 to the vCRE/CREB/Tax ternary complex. A study by Harrod et al (67) identified the region of Tax critical for binding to CBP/p300 as amino acids 81 – 95, which is between the domains for CREB binding (or NLS) and dimerization. Mutations in this domain (R82A, K85A, K88A, and V89A) failed to transactivate HTLV-1 transcription *in vivo* (67).

1.2d Major Tax Interactome

Tax relies on interaction with many cellular proteins to exert its oncogenic influence on infected cells. The Tax-interacting cellular proteins include transcription factors, post-translational regulators, mitogen-activated kinases (MAPKs), cell cycle-related proteins, and some transport proteins [reviewed in reference (68)]. Interactome is defined as a complete set of macromolecular interactions; however, it is beyond the scope of this dissertation to give a comprehensive review of proteins interacting with Tax. Therefore, only a few important Tax-interacting proteins are selected for a brief review as below.

In the context of Tax transactivation of HTLV-1 transcription, Tax interacts with CREB at the leucine zipper region, which enhances CREB dimerization and increases its affinity for binding vCREs (59). In addition, Siu et al (69) reported that Tax physically associates with CREB co-activator proteins called transducers of regulated CREB activity (TORCs) that includes three members, namely, TORC1/2/3. Moreover, p300 enhances the transcriptional coactivation of TORCs. Their studies revealed that the depletion of TORC1/2/3 abrogates Tax transactivation activity. Collectively, Tax activates HTLV-1 transcription optimally by interacting with CREB, CBP/p300 and TORCs.

The ternary complex formed by Tax, pCREB, and vCRE function as a platform for recruiting CBP/p300. It has been reported that pCREB binds the KIX domain of CBP via its kinase-inducible domain (KID) (70), however pCREB alone is insufficient for recruiting full-length CBP/p300 (25). Tax needs to be present on the vCRE, together with pCREB, for effective recruitment of the transcriptional

coactivators (25, 26). In addition, Tax directly binds the KIX domain of CBP (24, 71), but at a different surface within KIX from where pCREB binds (72).

Tax has also been reported to interact with the gene transcriptional repressor BCL6 (B-cell lymphoma 6) (73). The N-terminal poxvirus and zinc finger (POZ) domain of BCL6 is involved in its interaction with Tax. This protein-protein interaction enhances the repressive activity of BCL6, leading to down-regulation of Tax-induced HTLV-1 LTR transactivation and NF- κ B expression, which may contribute to the viral gene silencing during the latency period after initial HTLV-1 infection. This would allow HTLV-1-infected T-cells to avoid the host immune response.

1.3 The Multi-tasking Kinase: GSK-3

Previous unpublished *in vitro* studies in the Nyborg laboratory indicated that Tax physically interacts with GSK-3 β , resulting in strong inhibition of its kinase activity. The work described in this dissertation built upon this preliminary observation, and focused on defining the interaction between Tax and GSK-3 β , and elucidating the mechanism of kinase inhibition. This section introduces GSK-3 β , and defines its general role in cell signaling pathways.

Glycogen Synthase Kinase 3 (GSK-3) is a multifunctional serine/threonine kinase present in all eukaryotic cells. GSK-3 has two isoforms, namely, GSK-3 α (51 kDa) and GSK-3 β (47 kDa). These two isoforms share 97% amino acid sequence identity within their kinase domains (74). GSK-3 was initially discovered in studies examining glycogen metabolism where it phosphorylates and inhibits glycogen synthase. Later studies showed that GSK-3 is involved in a wide array of cell signaling, ranging from gene expression, protein translation, cell proliferation, cytoskeleton regulation, to cell death. It functions as a key regulatory switch that determines the output of numerous signaling pathways initiated by an array of stimuli (74-76).

GSK-3 β is the more widely studied and better characterized of the two isoforms. It is an atypical protein kinase in that it is active in resting cells. GSK-3 β is primarily regulated through inhibition of its kinase activity. Phosphorylation of Ser-9 at the N-terminus of GSK-3 β is inhibitory to the kinase activity, whereas the phosphorylation of Tyr-216 on the activation loop stimulates (~5 fold) the kinase activity. GSK-3 β regulates the function of many metabolic, signaling, and

structural proteins by phosphorylation. Among the signaling proteins regulated by GSK-3 β are many transcription factors, including CREB, heat shock factor-1, nuclear factor of activated T-cell (NFAT), myc, β -catenin, and NF- κ B (75). In contrast to other protein kinases, GSK-3 β has a peculiar preference for primed substrates, defined as proteins that have been previously phosphorylated by another kinase. Although there is not a strict consensus motif for substrates phosphorylated by GSK-3 β , many target proteins require prior phosphorylation at a serine or threonine by a priming kinase to form the phosphorylation motif (S/T-X-X-X-S/Tp) before efficient phosphorylation by GSK-3 β takes place. The transcription factor CREB is good example of a substrate that requires hierarchical phosphorylation by GSK-3 β . CREB is not a GSK-3 β substrate until it is first phosphorylated (or primed) by protein kinase A (PKA) or CaM kinase at Ser-133. The primary phosphorylation at Ser-133, together with residues neighboring Ser-133, provide the recognition motif (S¹²⁹-R-R-P_p-S¹³³) required for efficient phosphorylation by GSK-3 β at Ser-129. This sequential phosphorylation enables complex regulation of protein function.

Dysregulation of GSK-3 β has links to many human diseases. Elevated activity of GSK-3 β has been associated with type 2 diabetes and neurodegenerative diseases (77, 78), whereas aberrant inactivation of GSK-3 β has been implicated in several types of cancer (79).

1.3a The Structure of GSK-3 β

GSK-3 β is composed of 424 amino acids. The crystal structure of GSK-3 β was simultaneously determined by three different research groups (80-82). The

structure features a β barrel formed by seven anti-parallel β strands at the N-terminus (aa. 25–138) and an α -helical domain at the C-terminus (aa. 139–343). The basic residues Arg-96, Arg-180, and Lys-205 in the catalytic core of GSK-3 β form a positively-charged pocket that serves as the binding site for the priming phosphate present on primed substrates (80). The priming phosphate forms hydrogen bonds with Arg-96 of GSK-3 β . In addition, the activation loop (aa. 200–226) runs along the substrate binding groove and plays an important role positioning substrates in the catalytic domain for phosphorylation. A synthetic phospho-peptide, derived from GSK-3 β amino acids 4–14, inhibits GSK-3 β kinase activity. This inhibition occurs because the hydrogen bond formed between phospho-Ser-9 in the peptide and Arg-96 in the kinase domain of GSK-3 β excludes substrates from binding the catalytic domain of GSK-3 β (83).

The C-terminus of GSK-3 β features a hydrophobic groove formed by an α -helix (aa. 262 – 273) and an extended loop (aa. 285 – 299). This hydrophobic groove has been identified as binding site for both Axin (84) and FRAT1 (82). Therefore, Axin and FRAT1 competes for binding GSK-3 β through the hydrophobic groove. Phe-291 and Phe-293 on the extended loop of GSK-3 β are involved in the hydrophobic interaction with Axin and FRAT1 (84).

1.3b Regulation of GSK-3 β

Because GSK-3 β regulates a wide range of cellular processes, it is tightly regulated by upstream signaling through very complex mechanisms [see reference (75) for review]. GSK-3 β is primarily regulated through inhibitory phosphorylation of Ser-9 at its regulatory N-terminus. Phosphorylation at this site

causes a conformation change that leads to the formation of a hydrogen bond between phospho-Ser 9 and Arg-96 in the catalytically active kinase pocket (83). This conformational change in GSK-3 β prevents access of substrates into the catalytic domain, thus inhibiting the kinase activity of GSK-3 β (83). Several protein kinases have been identified that target Ser-9 in GSK-3 β , including p70 S6 kinase, p90Rsk, Akt, certain isoforms of PKC, and PKA (75, 85). Akt is implicated in the insulin receptor signaling pathway and directly phosphorylates Ser-9 of GSK-3 β upon activation by PI3K. Protein phosphatase 2A reactivates GSK-3 β by removing the inhibitory phosphate from Ser-9 (86). Many studies have focused on identifying the protein kinase signaling pathways that regulate the activity of GSK-3 β (87, 88).

Lithium is a selective inhibitor of GSK-3 β (113). Lithium induces phosphorylation of GSK-3 β at Ser-9 through activating the PI3K/Akt pathway, leading to inhibition of the kinase activity of GSK-3 β (89). In addition, lithium inhibits GSK-3 β *in vitro* by competing with magnesium for the cationic binding site. However, lithium is not specific to GSK-3 β , as it also inhibits other targets, including inositol monophosphatase (90) and other phosphomonoesterases structurally related to inositol monophosphatase (91, 92). GSK-3 β is the most sensitive protein kinase to lithium inhibition (85).

In opposition to the inhibitory modulation of GSK-3 β resulting from Ser-9 phosphorylation or ligand binding (e.g. Axin GID), Tyr-216 phosphorylation on the activation loop enhances its kinase activity. Dajani et al performed a quantitative GSK-3 β kinase assay using a phospho-primed peptide substrate, and they

observed an apparent stimulatory effect of Tyr-216 phosphorylation on GSK-3 β kinase activity, which was a 5-fold activation effect compared to the Tyr-216 unphosphorylated form of GSK-3 β (84). The physiological significance of Tyr-216 phosphorylation of GSK-3 β in mammalian cells is unclear, since phosphorylation at this site is constitutive in resting cells (93). Tyr-216 phosphorylation might facilitate substrate phosphorylation but is not strictly required for the kinase activity of GSK-3 β (81). This suggests that the role of Tyr-216 phosphorylation on GSK-3 β kinase activity is limited to enhancement, rather than direct activation.

1.3c Wnt Signaling

This section is designed to give readers background information on Axin, FRAT (frequently rearranged in advanced T-cell lymphoma), and the β -catenin destruction complex present in the Wnt signaling pathway. GSK-3 β in the destruction complex determines the output of the Wnt signaling by phosphorylating β -catenin. These signaling molecules are important for understanding the design and interpretation of the research project described in the second chapter.

The Wnts are a family of secreted glycoproteins that mediate embryogenesis, cell growth, differentiation, migration and fate (94). Deregulation of the Wnt signaling pathway is associated with many human cancers, in particular colorectal carcinoma, melanoma, and hepatocellular carcinoma (50, 95, 96). One of the pathways regulated by Wnts is the canonical Wnt pathway, which leads to activation of genes regulated by the Tcf/Lef family of architectural transcription factors (97-99). Cytoplasmic β -catenin, an effector molecule, is essential to

relaying the Wnt signals to the nucleus where gene expression patterns can be altered.

GSK-3 β plays a key inhibitory role in the Wnt signaling pathway. In unstimulated cells, GSK-3 β phosphorylates the N-terminus of β -catenin, targeting it for ubiquitylation and proteasome-regulated degradation, which is termed noncanonical Wnt pathway. Phosphorylation of β -catenin by GSK-3 β occurs in a destruction complex, which consists minimally of GSK-3 β , β -catenin, Axin and adenomatous polyposis coli (APC) (79). The Wnt signaling pathway inhibits GSK-3 β to pass on the signal from cell surface down to the nucleus through the effector molecule β -catenin. Both protein complex formation and phosphorylation are implicated in the mechanism of Wnt-mediated GSK-3 β inactivation (canonical Wnt pathway) (75). In response to Wnt signals, the cytoplasmic adaptor protein Dishevelled recruits the GSK-3 β -binding protein FRAT1 through an unknown mechanism (100), which replaces Axin from binding GSK-3 β in the destruction complex. As Axin is a substrate of GSK-3 β , dissociation of Axin from GSK-3 β results in the dephosphorylation of Axin (101), which further reduces its affinity for binding GSK-3 β . Dissociated GSK-3 β is inhibited by PKC or Akt phosphorylation of Ser-9 (102, 103). Collectively, the dissociation and inhibitory phosphorylation of GSK-3 β lead to the cytoplasmic stabilization of β -catenin and its nuclear translocation. β -Catenin binds Lef/Tcf transcription factors and activates target genes involved in cell growth, cell cycle regulation and cell development [reviewed in reference (99)].

1.3d Cellular Targets of GSK-3 β

GSK-3 β substrates play important roles in a wide range of cellular processes. Phosphorylation of these substrates by GSK-3 β is often inhibitory, as in the cases of glycogen synthase and β -catenin.

The phosphorylation of CREB at Ser-133 (pCREB) creates a consensus recognition site for subsequent phosphorylation by GSK-3 β at Ser-129. The first phosphorylation at Ser-133 enhances the DNA binding activity of CREB (104), although this result remains controversial. Additionally, Ser-133 phosphorylated CREB has been shown to bind the KIX domain of CBP/p300 (105-107), however, pCREB recruitment of the full length coactivators has been called into question (25). Few studies have addressed the functional effects of the secondary phosphorylation at CREB Ser-129 by GSK-3 β . Mutational analysis of CREB indicates that the mutation of Ser-129 \rightarrow Ala impaired the transcriptional activity of CREB in response to elevated cAMP levels (108). However, contradictory results on the activity of CREB following Ser-129 phosphorylation by GSK-3 β have been reported. Fiol et al found that GSK-3 β facilitated activation of CREB-regulated transcription in F9 cells (108). In contrast, Bullock and Habener provided evidence that phosphorylation of CREB by GSK-3 β attenuated PKA-induced CREB DNA binding activity (104). Consistent with the latter report, Grimes and Jope found that CREB transcriptional activity was inversely related to GSK-3 β activity in neuroblastoma cells, and that overexpression of GSK-3 β attenuated the transcriptional activity of CREB (109). What is needed now is a careful biochemical analysis of the effect of GSK-3 β phosphorylation of CREB on

the binding of the coactivators CBP/p300. Does Ser-129/133 phosphorylated CREB bind the KIX domain of CBP/p300 with higher affinity than Ser-133 phosphorylated CREB?

β -catenin belongs to the catenin family that also includes the α - and γ -catenin proteins. This transcription factor is mainly defined in the Wnt signaling, as described above in section 1.3c. The N-terminal region of β -catenin contains four highly conserved serine/threonine residues: Ser-45, Thr-41, Ser-37, and Ser-33. The protein kinase casein kinase I α is responsible for Ser-45 phosphorylation, which serves as a priming phosphate site for the processive phosphorylation of Thr-41, Ser-37, and Ser-33 by GSK-3 β (110-112). The phosphorylation of Ser-33 and Ser-37 by GSK-3 β triggers proteasome recognition and degradation of β -catenin. Tumorigenic mutations in β -catenin usually occur at these phosphorylation sites. These mutations are oncogenic, as they stabilize β -catenin by preventing proteasome-mediated degradation (96).

The NFAT (nuclear factor of activated T-cells) proteins are a family of transcription factors regulated by calcineurin (a Ca²⁺-dependent phosphatase) and protein kinases. NFAT proteins include five structurally similar isoforms, named NFAT1-5. The NFAT proteins contain a DNA-binding domain structurally related to the REL-family transcription factor, which enables NFAT to bind DNA, however, the DNA binding capacity is weak. Therefore, NFAT needs to associate with other transcription factors to bind target gene promoters (113).

NFAT proteins were initially characterized in Jurkat T-cells, but they are actually expressed in a many types of cells. NFAT plays an important role in immune response by regulating expression of the cytokine genes. In non-activated T-cells, NFAT stays in the cytoplasm as a heavily phosphorylated protein, however, it is rapidly dephosphorylated and activated by calcineurin in response to the calcium signaling. Activated NFAT translocates to the nucleus where it associates with activator protein 1 (AP-1) and other transcription factors to stimulate target gene transcription including interleukin 2 (IL-2) (114).

The transcriptional activity of NFAT is countered by kinases that phosphorylate NFAT and expose its nuclear export signal. These kinases can be categorized as priming, maintenance, and export kinases (113). Priming kinases such as casein kinase 1 (CK1) are required to phosphorylate NFAT before GSK-3 β phosphorylates and causes NFAT nuclear export and termination of NFAT target gene transcription. Maintenance kinases reside in the cytosol to prevent NFAT from nuclear entry. Therefore, GSK-3 β causes nuclear export of NFAT, and GSK-3 β inhibition leads to nuclear retention and activation of NFAT target genes (115, 116).

In addition to the aforementioned transcription factors, GSK-3 β regulates several proteins involved in the cytoskeleton, including microfilaments, intermediate filaments, and microtubules. Phosphorylation of these structural proteins controls their association with the cytoskeleton, which regulates polymerization, stability and arrangement of microtubules, and the organelle transport in the cytoplasm (117). The most widely studied of these structural

protein substrates of GSK-3 β are microtubule-associated proteins (MAPs). MAPs are primarily regulated by phosphorylation, therefore MAPs are main targets for kinases that are involved in microtubule regulation (118-121).

Tau, a protein predominantly expressed in neuronal axons, is a remarkably soluble neuronal MAP that normally functions to promote the assembly and stabilization of the microtubule cytoskeleton. Tau binds to microtubules in a phosphorylation-dependent manner, which contributes to the stability of microtubules and neuronal structure. The hyperphosphorylated tau has a reduced affinity for microtubules, which impairs its ability to promote microtubule assembly. Hyperphosphorylated tau is a major component in the paired helical filaments, which is a major building block of neurofibrillary lesions in Alzheimer's brains (122). Therefore, an increase in hyperphosphorylated tau levels may result in the destabilization of microtubules, impairment of axonal transport, and aggregation of paired helical filaments, leading to neuronal degeneration (122). Tau is primarily regulated by kinases and phosphatases. GSK-3 β has been shown to phosphorylate Tau on up to ten residues (122-125), which contributes to the neuropathogenesis of Alzheimer's disease when GSK-3 β is deregulated.

MAP2 is another microtubule-associated protein regulated by GSK-3 β phosphorylation (117). Only a subset of the phosphorylation sites on MAP2 has been identified and none have been well characterized. Kinases implicated in MAP2 phosphorylation are PKC, MARKs (MAP/microtubule affinity regulating kinases), and PDPKs (Proline-directed protein kinases) (126-129). It has been

suggested that MAP2 is extensively phosphorylated at Ser/Thr-Pro motifs by GSK-3 β , which leads to the dissociation of MAP2 from microtubules (117).

To this end, GSK-3 β exerts a critical influence on neuronal structure and cytoskeleton dynamics by phosphorylating the microtubule-associated proteins.

1.3e Cellular Proteins Interacting with GSK-3 β

Axin is a substrate of GSK-3 β and binds to the hydrophobic groove (formed by α -helix [amino acids 262 – 273] and the extended loop [amino acids 286 – 300]) close to the C-terminus of GSK-3 β (84). Phosphorylation of Axin enhances its binding to GSK-3 β . The crystal structure of GSK-3 β with Axin bound (PDB: 1O9U) published by Dajani et al in 2003 (84) indicated that a peptide named Axin GID (GSK-3 β interacting domain), derived from Axin amino acids 383 – 401, binds GSK-3 β mainly through hydrophobic interaction (Fig 1.4A). By direct association, the Axin GID peptide inhibits the kinase activity of GSK-3 β , whereas the full-length Axin does not (130). GSK-3 β in the destruction complex of the Wnt signaling pathway is primarily regulated by the regulatory binding protein FRAT1. A synthetic peptide named FRATtide corresponding to FRAT1 amino acids 188 – 226 binds and inhibits GSK-3 β activity toward non-primed substrates, but not primed substrates (82, 130) (Fig. 1.4B). The interaction of FRATtide and GSK-3 β blocks Axin from binding GSK-3 β , which further prevents Axin-dependent β -catenin phosphorylation (82).

The KSHV (Kaposi's Sarcoma-Associated Herpesvirus) viral protein LANA (Latency-Associated Nuclear Antigen) was recently found to interact with GSK-3 β

(131). Both the N-terminus and C-terminus of LANA are required for interaction with GSK-3 β . The region in LANA spanning amino acids 219 – 268 contains the phosphorylation site(s) for GSK-3 β . The other region located between amino acids 1112 – 1135 in the C-terminus of LANA is involved in the protein-protein interaction with GSK-3 β . The interaction region of LANA contains a low level amino acid sequence homology to Axin GID (132). Furthermore, the single-point mutation L1132 \rightarrow P renders LANA unable to interact with GSK-3 β . The results reported by Fujimuro et al in 2005 (131) indicated that LANA activates the β -catenin pathway through inhibiting and depleting cytoplasmic GSK-3 β . However, this conclusion is being challenged by a recent study published in 2009. Hagen found that LANA did not regulate the kinase activity of GSK-3 β , and the LANA-induced upregulation of β -catenin is independent of GSK-3 β (133).

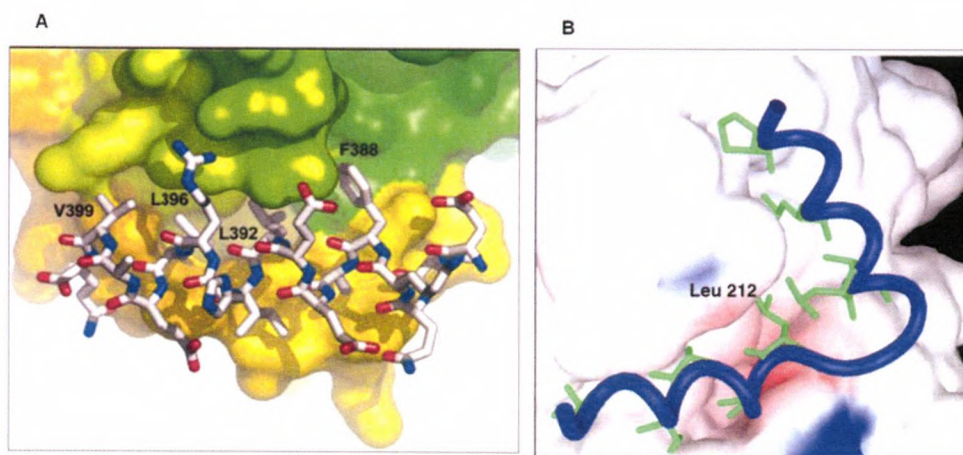


Figure 1.4. Axin GID and FRATtide bind to the same hydrophobic groove in GSK-3 β . (A) Axin GID (the stick model) packs into the hydrophobic groove of GSK-3 β (PDB: 1O9U). Adapted from reference (84). (B) Crystal structure of GSK-3 β and FRATtide demonstrates that FRAT binds to GSK-3 β in the same hydrophobic groove as Axin GID binds (PDB: 1GNG). Adapted from reference (82).

1.4 Thesis Research Objectives and Significance

This research project was spawned from the initial discovery made by Aida Ulloa, an MS student in the Nyborg laboratory, that HTLV-1 Tax directly interacts with GSK-3 β , and inhibits its kinase activity directed toward Ser-133 phosphorylated CREB. The objective of my thesis project was to characterize the protein-protein interaction between Tax and GSK-3 β , and characterize the downstream impact of GSK-3 β inhibition by Tax. HTLV-1-associated malignancy is likely due to the interaction between Tax and a variety of transcription factors and critical cell signaling regulators. Because GSK-3 β is a critical regulator in determining cell fate, investigating the interaction between Tax and GSK-3 β may contribute to understanding HTLV-1-associated leukemogenesis.

To identify the interaction domains in both Tax and GSK-3 β , I performed a sequence alignment between GSK-3 β interacting proteins and full-length Tax. Two GSK-3 β -interacting ligands appeared to be most interesting: Axin GID and FRATtide. These two short peptides derive from full-length Axin and FRAT1, respectively, and both peptides inhibit GSK-3 β (82, 84, 130, 134, 135). The amino acid sequence alignment indicates a significant homology between Tax amino acids 185 – 205 and Axin GID and FRATtide. From these important observations, I hypothesize that this short region of Tax (aa. 185 – 205), which I called the putative Tax GSK-3 β -interacting domain, or Tax GID, is responsible for the direct interaction with GSK-3 β and the resultant kinase inhibition. I constructed two deletion mutants of GSK-3 β based on its crystal structure (84), and the results of my computer-aided comparative modeling and docking tests.

The α -helix (aa. 262 – 273) and the extended loop (aa. 285 – 300) were deleted and characterized for interaction with Tax by co-immunoprecipitation (Co-IP) assays.

To study the protein-protein interaction *in vivo*, I first performed Co-IP assays using 293T cells cotransfected with a Tax expression plasmid and HA-tagged GSK-3 β . The Co-IP data suggested that Tax interacts with GSK-3 β *in vivo*, which is in agreement with our *in vitro* data showing direct association of Tax and GSK-3 β .

I also focused on the interaction between GSK-3 β and the putative Tax GID peptide. My study employed *in vitro*, cell-based assays and computational simulation to achieve the objectives, including GST pull-down, *in-vitro* GSK-3 β kinase assay, protein structural modeling, and protein-ligand docking. My strategy was to construct point mutations in the putative Tax GID region in the full-length Tax and the hydrophobic groove of GSK-3 β where Tax was hypothesized to bind. Site-directed mutagenesis in Tax was performed for expression in bacteria or mammalian cells. The purified Tax wild-type and mutant proteins were used for GST pull-down assays. Co-IP assays were performed to study the Tax-GSK-3 β interaction in cells. To further pinpoint the interaction regions in Tax and GSK-3 β , Tax GID was cloned and expressed in bacteria or mammalian cells for *in vitro* GSK-3 β kinase assays or Co-IP assays.

The data presented herein indicate that: 1) HTLV-1 Tax inhibits GSK-3 β kinase activity through direct interaction, 2) A peptide deriving from the putative

Tax GID inhibits GSK-3 β , and 3) Tax has no effect on the activation of the β -catenin and NFAT pathways.

❖ *Significance*

Our discovery that Tax inhibits GSK-3 β *in vitro* through physical interaction, leading to reduced phosphorylation of both primed and non-primed substrates, may represent a newly described strategy of HTLV-1 to modulate the numerous cell signaling pathways regulated by GSK-3 β . Many of these signaling pathways are critical to cell survival and apoptosis, which if deregulated may contribute to cell transformation caused by HTLV-1 infection. Specifically, Tax may inhibit GSK-3 β phosphorylation of β -catenin by direct interaction, which would be oncogenic. Furthermore, CREB is a well-characterized substrate of GSK-3 β that plays an important role in driving viral and cellular gene expression. Bullock and Habener (104) found that the DNA binding activity of CREB is enhanced by phosphorylation at Ser-133, while the sequential phosphorylation of CREB Ser-129 by GSK-3 β attenuates its DNA binding activity. It is likely that Tax inhibits GSK-3 β *in vivo* to ensure the availability of transcriptionally active pSer-133 CREB for expressing a large body of proto-oncogenes.

Chapter 2 Molecular Characterization of GSK-3 β Inactivation by HTLV-1 Tax

This chapter describes a study on characterization of the protein-protein interaction between GSK-3 β and HTLV-1 Tax and the mechanism of Tax inhibition of GSK-3 β kinase activity.

2.1 Abstract

The human T-cell leukemia virus type 1 (HTLV-1) encodes a viral oncoprotein termed Tax, which plays a major role in transforming HTLV-1-infected cells. Tax is a potent transcriptional activator that stimulates HTLV-1 viral and cellular gene transcription. In addition, Tax disrupts a number of cell signaling pathways involved in cell growth and survival. Glycogen synthase kinase-3 β (GSK-3 β) is a ubiquitously expressed serine/threonine kinase present in all eukaryotic cells, which functions as a critical regulator of a wide range of cell signaling pathways. As GSK-3 β is constitutively active in resting cells, it is primarily regulated through inhibition. Ser-9 phosphorylation is inhibitory to the kinase activity of GSK-3 β . Deregulation of GSK-3 β has been linked to many human diseases such as Alzheimer's disease and cancers.

It has been reported in Aida Ulloa's thesis that Tax inhibits GSK-3 β kinase activity toward both primed and non-primed substrates through direct association. To delineate the protein-protein interaction between Tax and GSK-3 β , we compared the amino acid sequence of Tax with a well-characterized short peptide deriving from the GSK-3 β interacting domain (GID) of Axin, and found that Tax contains a notable amino acid sequence homology to Axin GID. The region spanning Tax amino acids 185 – 205 has 24% sequence identity and 19% similarity with Axin GID. We named this region the putative Tax GID. We characterized the putative Tax GID biochemically, and discovered that a longer peptide (Tax aa. 138 – 205) of the putative Tax GID strongly inhibits GSK-3 β kinase activity *in vitro*. Bioinformatics computation was used to predict the secondary structure of the Tax GID, which was further used in our docking test to identify a potential binding interface in GSK-3 β . This was tested by GST pull-down and Co-IP assays using point and deletion mutants. In addition, the effects of Tax-GSK-3 β interaction on the downstream β -catenin and NFAT pathways were characterized by luciferase reporter assays. However, unexpectedly, we observed that Tax expression has little effects on β -catenin and NFAT transcriptional activation.

2.2 Introduction

Human T-cell leukemia virus type 1 (HTLV-1) is a human retrovirus that causes adult T-cell leukemia (ATL) and the neurodegenerative disease tropical spastic paraparesis/HTLV-1-associated myelopathy (TSP/HAM) (136). The viral oncoprotein Tax is encoded by the *pX* region of the HTLV-1 viral genome. Tax is a potent activator that stimulates HTLV-1 and cellular gene transcription (137, 138). Tax activates viral gene expression by interacting with CREB, and together they recruit CBP/p300 to form a multiprotein complex on the regulatory elements known as cAMP response elements (CREs) in the HTLV-1 LTR. In addition, Tax disrupts a number of cell signaling pathways to alter cellular gene expression patterns, and thus plays a major role in transforming cells (139). By deregulating signal transduction pathways such as the NF- κ B and the phosphoinositide 3-kinase (PI3K) pathways, Tax stimulates transcription of many cellular genes, thereby promoting cell cycle progression, proliferation and cell survival.

Glycogen synthase kinase-3 is a ubiquitous serine/threonine kinase expressed as α and β isoforms in eukaryotes and has been implicated in cell metabolism, growth, gene transcription, cell cycling, cytoskeleton dynamics, apoptosis, and cell fate determination (75, 79). GSK-3 β has a mass of 47 kDa, whereas GSK-3 α has a mass of 51 kDa. The kinase domains of the two isoforms share 98% sequence identity, the size difference is due to the glycine-rich extension at the N-terminus of the α isoform (79). GSK-3 β is the more widely studied isoform. Unlike most other protein kinases, GSK-3 β is constitutively active in senescent cells, and its regulation occurs primarily through inhibitory

phosphorylation of Ser-9 at the N-terminus by kinases such as Akt and p90RSK (79, 140). The phosphorylated N-terminus acts as a pseudosubstrate that competes with real substrates for binding to the phosphate-binding site located in the catalytic pocket of GSK-3 β (83). GSK-3 β has a peculiar preference for primed substrates previously phosphorylated by another kinase. Biochemical studies of GSK-3 β indicate that the kinase activity of GSK-3 β differs toward phosphorylating primed and non-primed substrates. GSK-3 β has a higher phosphorylation efficiency toward primed substrates such as pCREB (74, 80, 81, 83, 134).

GSK-3 β is an essential component in the Wnt signaling pathway by forming a destruction complex with Axin/conductin, β -catenin and Adenomatous Polyposis Coli protein (APC). Axin functions as a scaffolding protein that brings GSK-3 β and β -catenin in close proximity for GSK-3 β to phosphorylate β -catenin and target it for proteasomal degradation. Axin phosphorylation by GSK-3 β enhances its binding to GSK-3 β . However, GSK-3 β is inhibited in response to Wnts, causing dephosphorylation of substrates such as Axin and β -catenin (141, 142). Stabilized β -catenin translocates to the nucleus where it associates with the T-cell factor and lymphoid enhancer factor (Tcf/Lef) to form a transcription complex that activates Wnt target genes (e.g., cyclin D1 and c-Myc) (47, 48). Aberrant inhibition of GSK-3 β is found in many human cancers (96). Furthermore, elevated activity of GSK-3 β is associated with such diseases as type 2 diabetes, neurodegenerative diseases, and bipolar disorders (77, 143).

Lithium is a direct inhibitor of GSK-3 β by competing with magnesium for the cationic binding site of GSK-3 β (144). Moreover, lithium inhibits GSK-3 β *in vivo* by facilitating Akt phosphorylation of GSK-3 β Ser-9 and suppressing protein phosphatase 1 that activates GSK-3 β by dephosphorylating phospho-Ser-9. Robust and rapid Ser-9 phosphorylation has been observed in 293T cells treated with lithium (130). Two short peptides, named Axin GID and FRATtide, respectively derived from Axin and FRAT1, have been reported to bind and inhibit GSK-3 β (82, 84, 145). In addition, the latency-associated nuclear antigen (LANA) of Kaposi's sarcoma-associated herpesvirus (KSHV) contains a low-level amino acid homology domain to the Axin GID, through which LANA interacts with GSK-3 β (131).

In this study, we present evidence for a physical association between Tax and GSK-3 β *in vivo*, which extends our *in vitro* data showing Tax-GSK-3 β interaction reported in Aida Ulloa's thesis. Furthermore, our *in vitro* GSK-3 β kinase assays demonstrated that a peptide derived from Tax amino acids 138 – 205 inhibits GSK-3 β kinase activity. We also found that Tax is phosphorylated by GSK-3 β *in vitro*, although the phosphorylation efficiency is low compared to CREB. This suggests that Tax may be a physiological substrate for GSK-3 β .

2.3 Results

2.3a Tax inhibits GSK-3 β via direct interaction.

We set out to investigate the possible interaction between Tax and GSK-3 β . Previous unpublished protein-protein interaction assays in the Nyborg laboratory showed that Tax directly interacts with GSK-3 β *in vitro*. Furthermore, Tax strongly inhibits GSK-3 β kinase activity toward both primed (phosphorylated CREB, or pCREB) and non-primed (cJun) substrates in a concentration-dependent manner (see Aida Ulloa's M.S. thesis for details).

We were interested in determining whether Tax associates with GSK-3 β *in vivo*. We performed co-immunoprecipitation (Co-IP) assays in 293T cells cotransfected with expression plasmids for Tax and HA-tagged GSK-3 β . Whole cell extracts were prepared, followed by immunoprecipitation with anti-Tax or anti-HA antibody. The presence of HA-GSK-3 β and Tax in the immune complex was analyzed by Western blot. Figure 2.1A shows the presence of Tax in the complex with GSK-3 β , immunoprecipitated with the anti-HA antibody. The Tax-GSK-3 β interaction was confirmed by the reciprocal Co-IP assays (Figure 2.1B). Extending the GST pull-down assay results, the Co-IP results indicate that Tax physically associates with GSK-3 β *in vivo*.

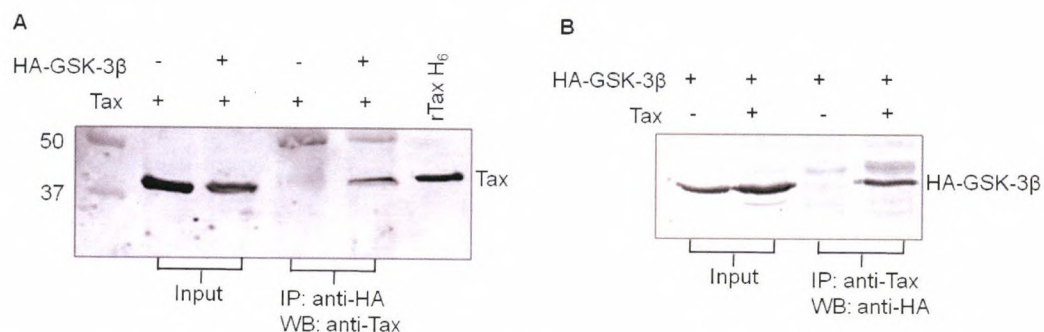


Figure 2.1. Tax interacts with GSK-3 β *in vivo*. Whole cell extracts (WCE) were prepared from 293T cells transfected with HA-GSK-3 β in the presence or absence of Tax. (A) WCE was immunoprecipitated (IP) with anti-HA antibody, followed by western blot (WB) analysis using anti-Tax antibody. Purified recombinant Tax (rTaxH₆) protein was loaded as a control. Molecular weight standards (in kDa) are labeled to the left of the WB image. (B) WCE was immunoprecipitated with anti-Tax antibody, followed by western blot analysis using anti-HA antibody.

2.3b Identification of GSK-3 β interacting domain in Tax.

The discovery that Tax binds and inhibits GSK-3 β led us to investigate the molecular basis for this interaction. To study the mechanism of the protein-protein interaction between Tax and GSK-3 β , we compared the amino acid sequence of full-length Tax and the two GSK-3 β -interacting proteins: Axin and FRAT1 (82, 84). When the Wnt signaling pathway is activated by the binding of Wnt glycoproteins to the receptor on cell surface, FRAT1 mediates the dissociation of GSK-3 β from Axin. A peptide, termed FRATtide, derived from FRAT1 amino acids 188 – 226, binds and inhibits GSK-3 β . The Axin GID (GSK-3 β interacting domain), an amphipathic α -helix of Axin (aa. 383 – 401), binds to a hydrophobic groove near the C-terminus of GSK-3 β (aa. 262 – 299) (84). The Axin GID binding site in GSK-3 β overlaps with that for FRATtide, thus they are mutually exclusive for binding GSK-3 β . A sequence alignment between the Axin GID, FRATtide, and Tax is shown in figure 2.2. The alignment reveals striking sequence similarity and identity in the region of Tax spanning amino acids 185 – 205. We hypothesized that this small region of Tax, termed putative Tax GID, is involved in the molecular interaction with GSK-3 β , which leads to inaccessibility of the catalytic domain of GSK-3 β to its substrates (Figure 2.3). We first wanted to test whether the putative Tax GID is involved in binding to GSK-3 β by constructing single-point mutations within this region. The amino acids selected for site-directed mutagenesis were based on the sequence homology between Tax and Axin GID, and the published studies on Axin GID (84, 130, 131). We constructed a series of single-point Tax mutants, and characterized each mutant

by GST pull-down assays. However, none of them compromises the interaction with GSK-3 β . Therefore, we decided to make more extensive mutations in Tax. Five amino acid substitutions were introduced into Tax at the following positions: E193 \rightarrow A, L194 \rightarrow A, L195 \rightarrow A, K197 \rightarrow A, and I198 \rightarrow A. We call this Tax mutant Tax 5A. Based on the sequence homology, the Tax residues Leu-194, Lys-197, and Ile-198 are analogous to Leu-392, Arg-395, and Leu-396 in Axin GID. It is worth to point out that Leu-392 and Leu-396 are critical for the hydrophobic interaction between Axin GID and GSK-3 β . In addition, Arg-395 in Axin GID hydrogen bonds to Asp-264 in GSK-3 β (84). It is possible that the analogous Tax residues make similar interactions with GSK-3 β . Figure 2.4A shows the schematic location of the mutated residues in Tax 5A. The Tax 5A mutant was purified along with wild-type Tax, as shown in figure 2.4B. GST pull-down assays were performed to characterize Tax 5A for its binding to GSK-3 β . The Tax 5A mutant exhibited diminished interaction with GSK-3 β (Fig. 2.4C), suggesting that the putative Tax GID region is important for interaction with GSK-3 β .

```

185-NVPYKRI EELLYKI SLTTGAL-205 Tax
          *  *  * * * | |
380-EVRVEPQKFAEEL IHRLEAVQRTR-403 Axin GID
          * | | | | | * | |
188-SQPETRTGDDDPHRL LQQLVLSGNLI KEAVRRLHSRLQ-226 FRATtide

```

Figure 2.2. Amino acid sequence alignment between Tax, human Axin GID and FRATtide indicates notable sequence homology. (*) denotes identity, and (|) denotes similarity. The highlighted region shows 43% sequence similarity and 43% sequence identity between Tax aa. 192 – 198 and Axin GID.

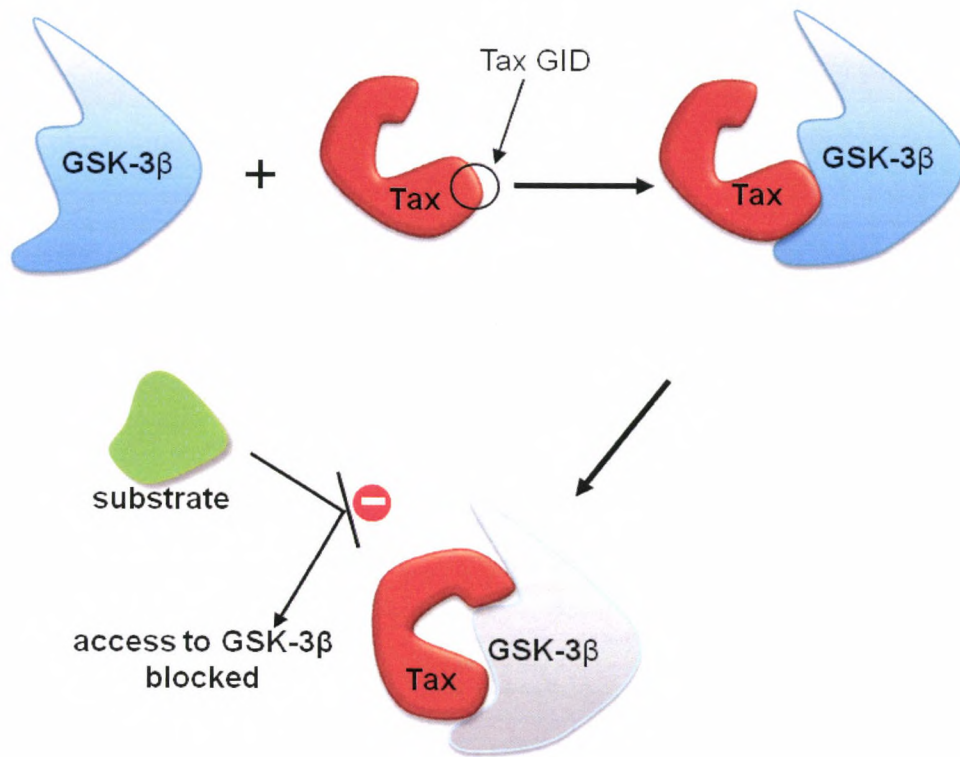


Figure 2.3. Hypothetical model depicting the mechanism of Tax inhibition of GSK-3 β kinase activity. Tax interacts with GSK-3 β through its putative GID region (aa. 185 – 205), which provides docking interaction for full-length Tax to block the access of substrates to the catalytic domain of GSK-3 β , thus preventing GSK-3 β from phosphorylating its substrates.

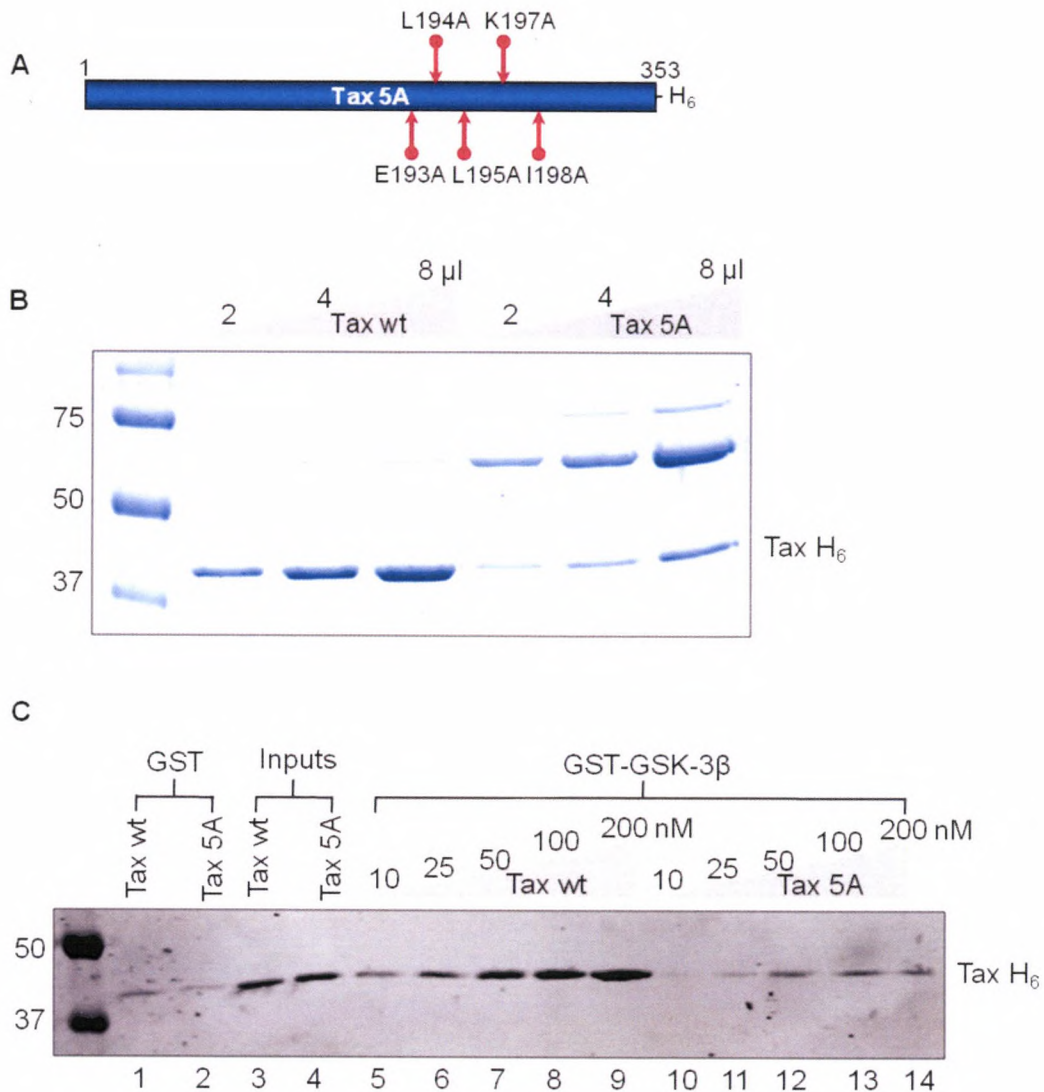


Figure 2.4. Design and purification of Tax GID mutant that shows diminished interaction with GSK-3 β . (A) Schematic diagram of full-length Tax in which the five labeled amino acid residues were mutated to alanines. (B) The Tax 5A mutant was purified along with wild-type (wt) Tax. The purified proteins were subjected to SDS/PAGE analysis and coomassie blue staining as shown. Three different amounts were analyzed for each protein, as indicated. (C) Tax 5A mutant shows diminished interaction with GSK-3 β . Western blot analysis of a GST pull-down assay was performed to compare wt and Tax 5A mutant for binding GST-GSK-3 β . Western blot membrane was probed with an anti-His antibody. Input wt Tax and 5A mutant (each contains 2.5% of the highest amount used in this assay) are shown in lanes 3 and 4, respectively.

2.3c Tax GID inhibits GSK-3 β .

To further characterize the Tax-GSK-3 β interaction, we wanted to express and purify the putative Tax GID (Tax aa. 185 – 205) from bacteria. However, we found that 43% of the Tax GID residues are hydrophobic, which may have solubility issue in aqueous media, making it difficult to purify. To make it easier, we decided to purify the Tax GID as a longer peptide (Tax aa. 138 – 205, named Tax GID₁₃₈₋₂₀₅) from bacteria, as a longer peptide is more likely to be structured than the short Tax GID₁₈₅₋₂₀₅. We first constructed a hexahistidine-tagged Tax GID₁₃₈₋₂₀₅ plasmid for expression. However, the induced His₆-Tax GID₁₃₈₋₂₀₅ remained insoluble. Therefore, we switched to using a GST tag to improve the peptide solubility (Fig 2.5A). We were able to purify the longer Tax GID₁₃₈₋₂₀₅ peptide as a GST fusion protein (Fig. 2.5B).

The purified GST-Tax GID₁₃₈₋₂₀₅ was first examined for GSK-3 β inhibition by *in vitro* kinase assays with GST as negative control. Full-length Tax and lithium were used as positive controls for GSK-3 β inhibition. Interestingly, Tax GID₁₃₈₋₂₀₅ inhibited GSK-3 β phosphorylation of pCREB in a concentration-dependent manner (Fig. 2.5C). As expected, both Tax and lithium strongly inhibited GSK-3 β kinase activity. The kinase assays were repeated three times, which were then quantified and plotted in figure 2.5D.

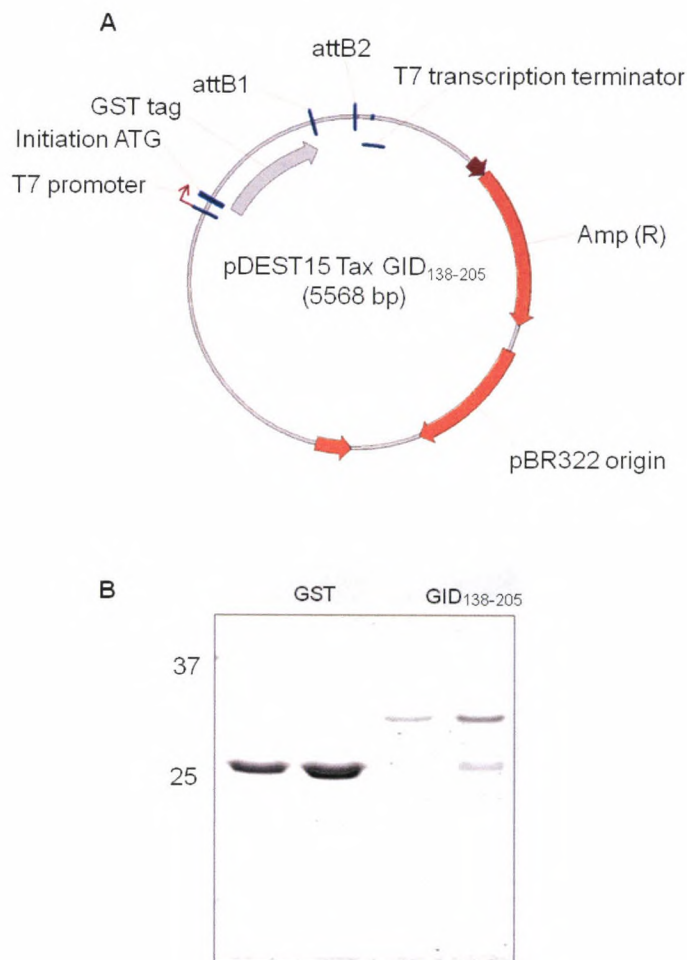


Figure 2.5. (A) The GST-TaxGID₁₃₈₋₂₀₅ expression plasmid was constructed by using the Gateway cloning system. Tax DNA fragment comprising amino acid residues 138 – 205 was cloned and inserted between the *attB1* and *attB2* sites of the pDEST 15 vector to produce the N-terminal GST fusion construct pDEST15/TaxGID₁₃₈₋₂₀₅. (B) The purified GST-tagged Tax GID₁₃₈₋₂₀₅ and GST proteins were analyzed on SDS-PAGE with coomassie stain.

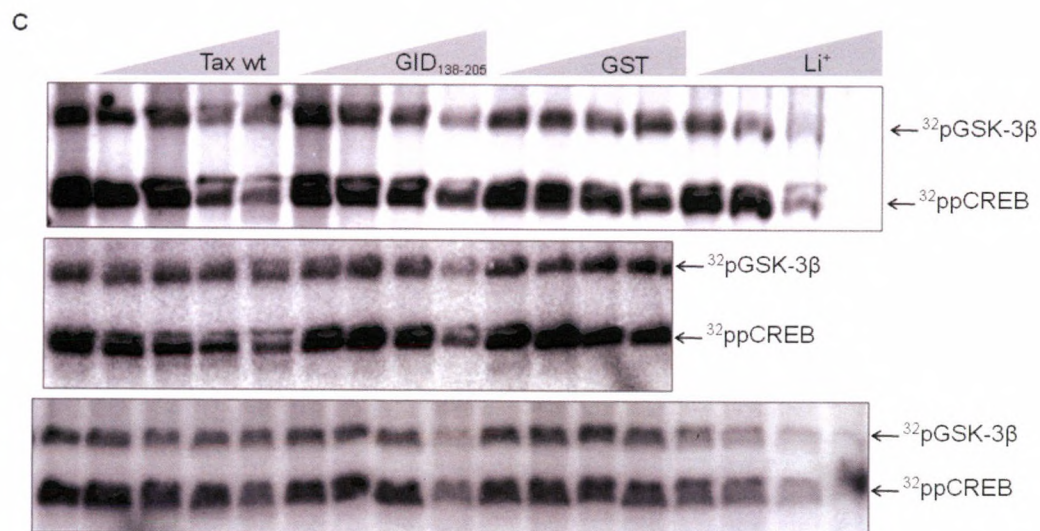


Figure 2.5C. Tax GID₁₃₈₋₂₀₅ inhibits GSK-3β kinase activity *in vitro*. Purified recombinant GST-fused Tax GID₁₃₈₋₂₀₅, Tax, and GST proteins were used in the GSK-3β *in vitro* kinase reactions at the concentrations of 45, 90, 175, and 350 nM. Increasing concentrations (10, 20, 50, and 100 mM) of LiCl were used as positive controls for inhibiting GSK-3β. Each reaction contains 4.15 nM of GST-fused GSK-3β kinase and pCREB (25 nM). Reactions were performed in the presence of [γ -³²P]ATP, as described in materials and methods. The kinase assays shown here include three independent experiments.

D

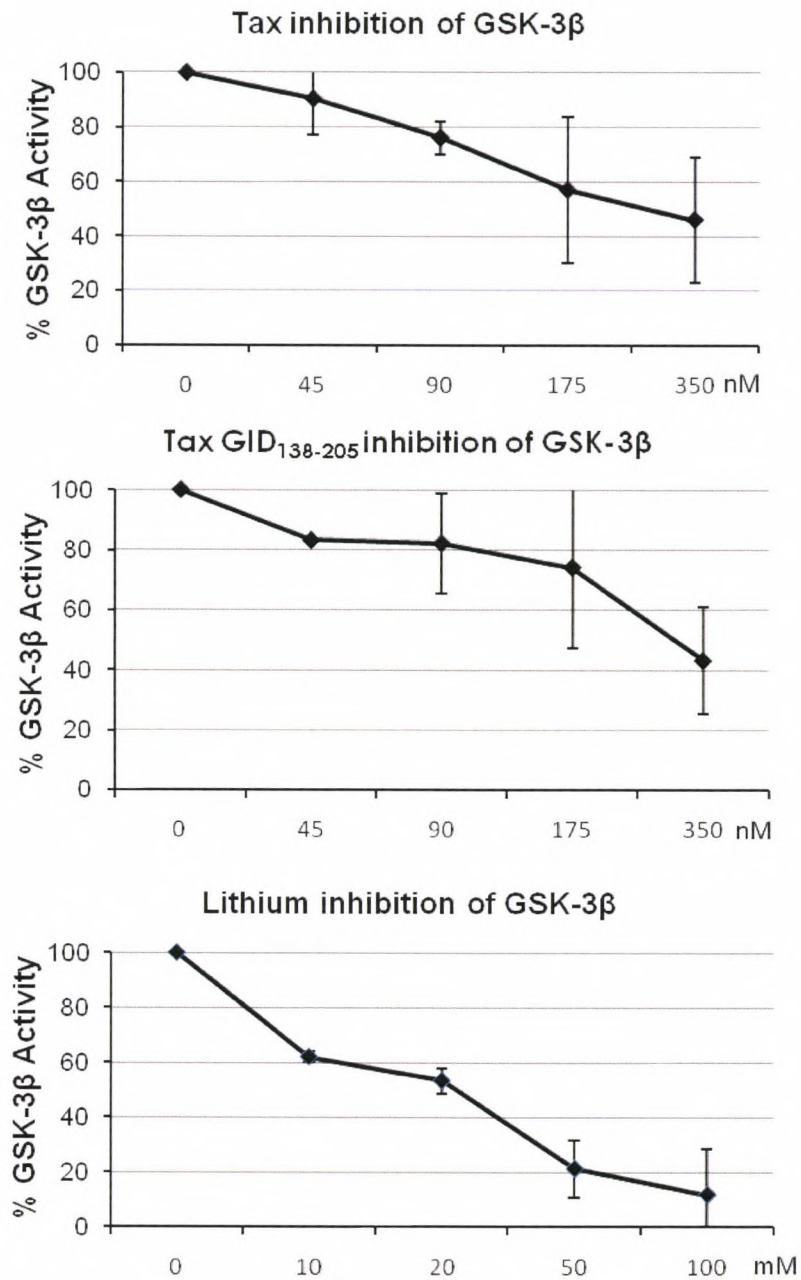


Figure 2.5D. Quantitation of GSK-3β inhibition. The inhibition of GSK-3β as shown in (C) was quantified by measuring the incorporation of radiolabeled phosphate into ppCREB. Relative GSK-3β kinase activity was measured by setting the untreated phosphorylation reaction (lane #1 without inhibitors in each panel) to 100%. Error bars denote the standard deviation of the relative change of GSK-3β activity among the three independent experiments.

We next considered the possibility that the purified Tax or Tax GID₁₃₈₋₂₀₅ proteins may contain contaminating phosphatase(s) that targets CREB-pSer-133 and/or pSer-129, thus giving the appearance of kinase inhibition. We reasoned that even a small amount of contaminating phosphatase would remove the priming phosphate from CREB, making CREB an unsuitable substrate for GSK-3 β . Therefore, we designed and implemented phosphatase assays, in which we tested whether Tax, or GST-Tax GID₁₃₈₋₂₀₅ can remove the priming phosphate from pSer-133 of CREB. As shown in figure 2.6A, the phosphorylation level of ³²pCREB with ³²pSer-133 was not significantly reduced after adding the indicated proteins. To confirm this result, we did a similar phosphatase assay with cold pCREB by using a pSer-133 CREB phospho-specific antibody in the Western blot shown in figure 2.6B, which consistently shows that pCREB did not get dephosphorylated. Since pCREB is additionally phosphorylated by GSK-3 β at Ser-129 in the *in vitro* kinase assays, we wanted to examine whether the purified Tax or Tax GID₁₃₈₋₂₀₅ proteins have contaminating phosphatase targeting pSer-129 of CREB. For this reason, we used double-phosphorylated CREB (³²ppCREB with ³²pSer-129 and pSer-133) in the phosphatase assays as shown in figure 2.8C. We observed no significant reduction of the phosphorylation level of ppCREB. Taken together, neither Tax nor Tax GID₁₃₈₋₂₀₅ has significant contaminating phosphatase against pSer-133 or pSer-129 of CREB. This observation further suggests that Tax or Tax GID₁₃₈₋₂₀₅ inhibition of GSK-3 β is not due to dephosphorylation of ppCREB or pCREB in the GSK-3 β *in vitro* kinase assays, rather, they directly inhibit GSK-3 β kinase activity.

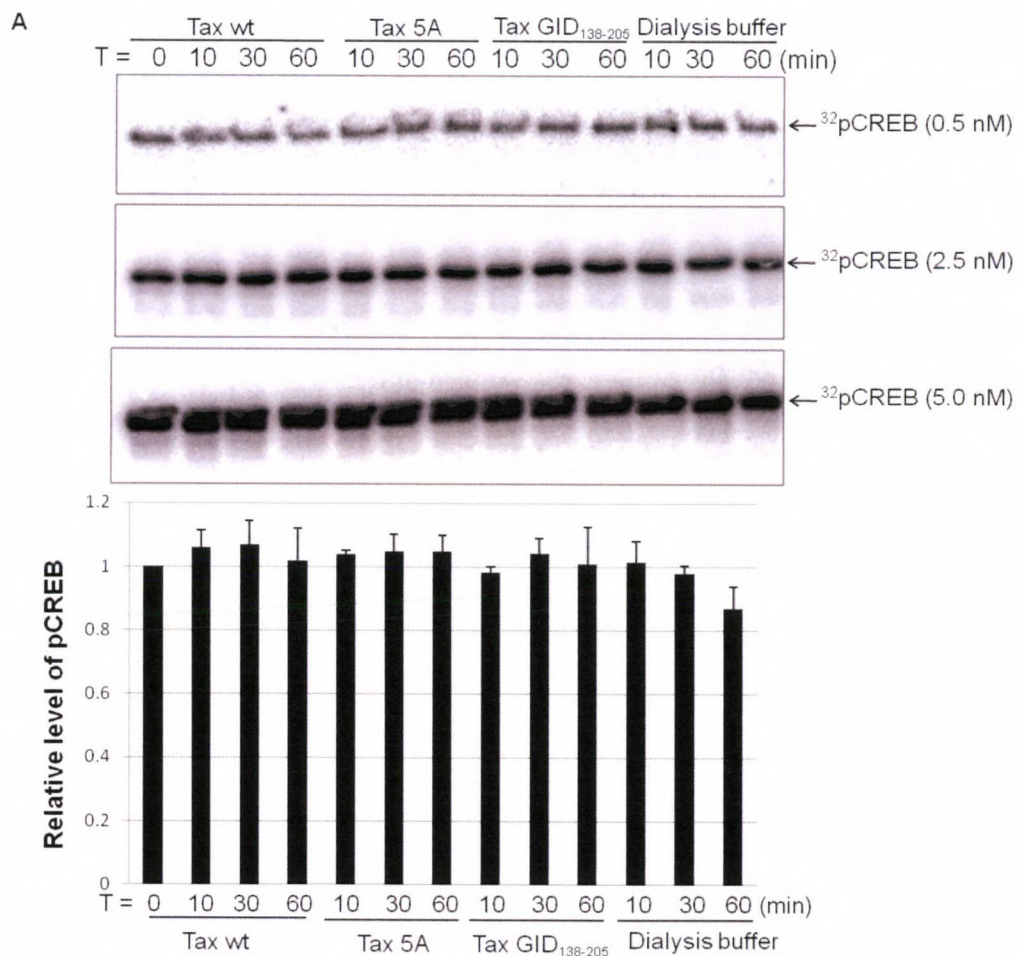


Figure 2.6. Examination of wild-type Tax, Tax 5A mutant, and GST-fused Tax GID₁₃₈₋₂₀₅ for contaminating phosphatase against CREB-pSer133. (A) Purified wild-type Tax, Tax 5A or Tax GID₁₃₈₋₂₀₅ were incubated at 30 °C with radiolabeled ³²pSer133 CREB (³²pCREB) for the indicated times. Three different concentrations of pCREB were used as indicated to the right of each panel. The time-course mean intensity of ³²pCREB in each reaction was measured, and the relative intensity was determined by setting the zero time point (lane 1) in each panel to 1, which is plotted in the bottom panel.

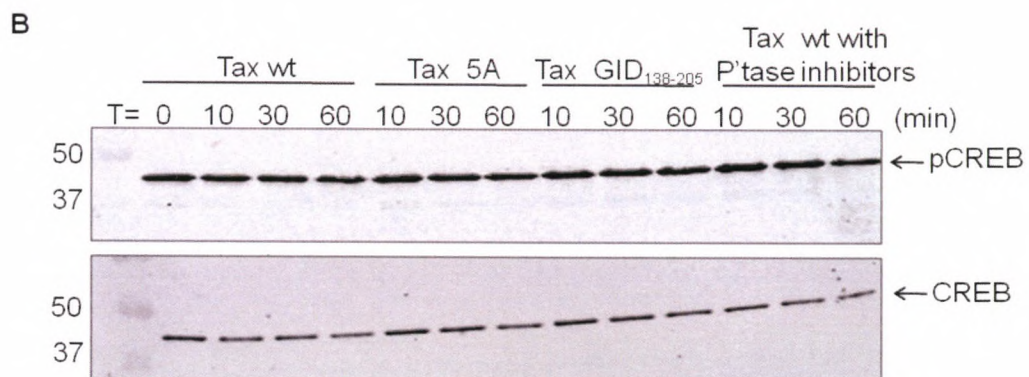


Figure 2.6B. A similar time-course phosphatase assay was performed as described in (A) with 25 nM of cold pCREB, which was then analyzed by Western blot with phospho-Ser133 and regular CREB antibodies. P'tase: phosphatase.

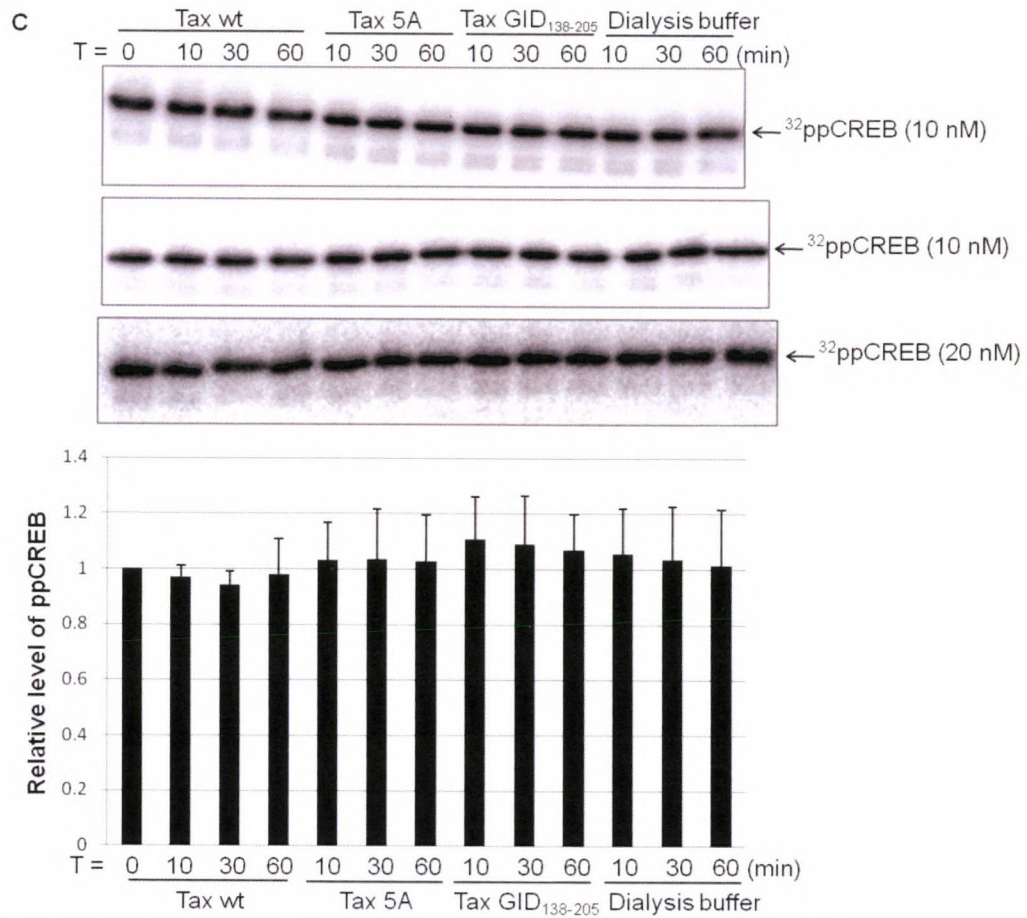


Figure 2.6C. Wild-type Tax, Tax 5A mutant, and GST-fused Tax GID₁₃₈₋₂₀₅ proteins do not have significant contaminating phosphatase against CREB-pSer129. The purified proteins as indicated were incubated with ³²pCREB (³²pSer129 and pSer133) for the indicated times. Two different amounts of ³²pCREB were used as indicated to the right of each panel. The time-course mean intensity of ³²p-CREB in each reaction was measured, and relative band intensity was determined by setting the zero time point (lane 1) to 1 in each panel, which is plotted in the lower panel. Error bars denote the standard deviation of the relative intensities from the three independent experiments.

2.3d Bioinformatics predictions and experimental analysis of the Tax-GSK-3 β interaction.

Having shown that both Tax and Tax GID₁₃₈₋₂₀₅ inhibit GSK-3 β , we wanted to know where Tax binds on the surface of GSK-3 β . Although the crystal structure of GSK-3 β has been solved (80-82), the challenge for addressing this problem results from the absence of the crystal structure of Tax. We have employed bioinformatics tools to predict the secondary structure of the putative Tax GID₁₈₅₋₂₀₅ and its interaction with GSK-3 β . Comparative homology modeling can be used to approximate three-dimensional (3D) structure of a target protein for which only the primary sequence is known, given an empirical 3D template that has > 30% sequence identity. It has been reported that comparative modeling based on more than 50% identity tends to have comparable accuracy to a low-resolution x-ray structure in terms of the main-chain carbon atoms (146). Based on the amino acid sequence alignment between Tax and Axin GID, as shown in figure 2.2, we used the published Axin GID structure (PDB: 1O9U, chain B) (84) as a template for modeling the secondary structure of the putative Tax GID using the SWISS-MODEL server (147-149). The predicted secondary structure of Tax GID is an α -helix as shown in figure 2.7A. We then performed a theoretical docking test with the predicted Tax GID structure as a ligand of stationary GSK-3 β molecule by using the 3D Dock software suite (see <http://www.bmm.icnet.uk/docking>). Figures 2.7B and 2.7C show the hydrophobic groove of GSK-3 β as the lowest energy binding site of Tax GID.

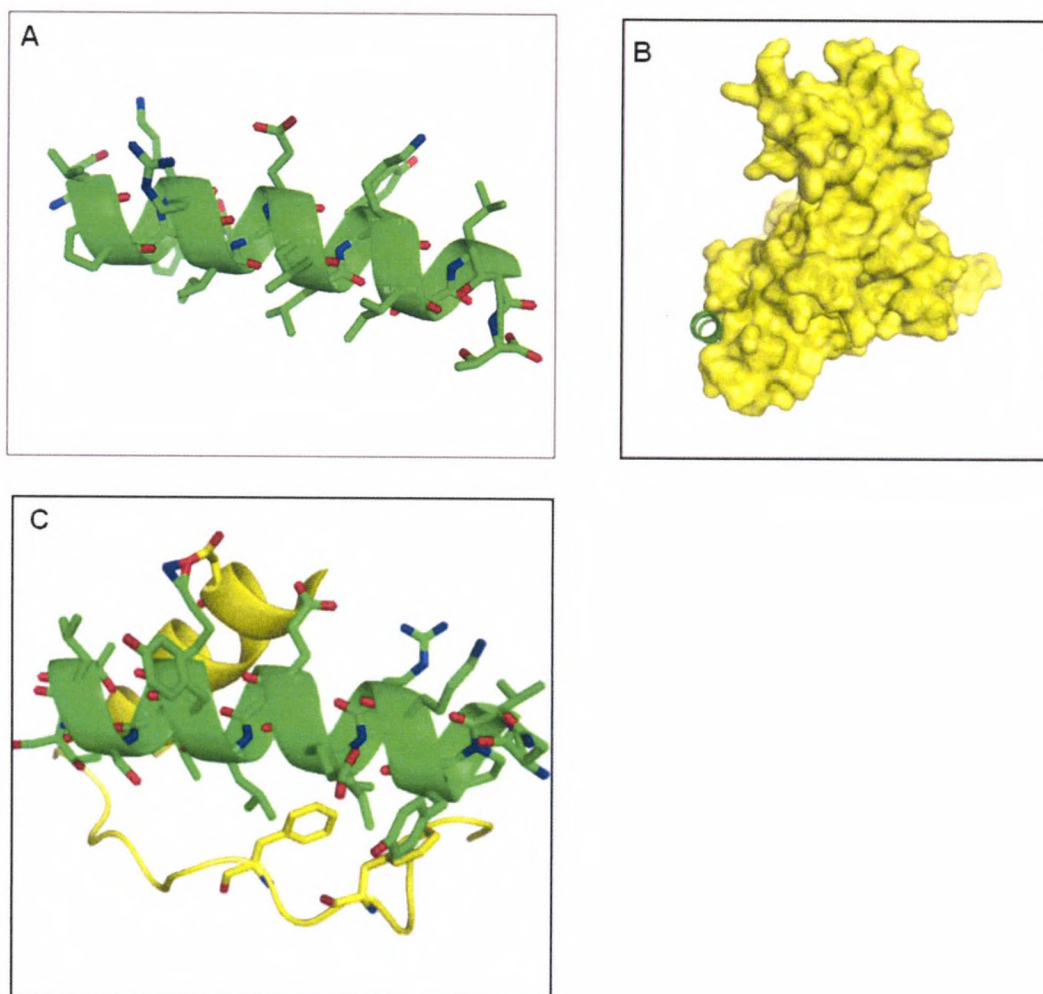


Figure 2.7. Computer-aided modeling of the Tax-GSK-3 β interactions. (A) Putative Tax GID (aa. 185 – 205) protein structure generated via comparative modeling using the Axin GID as a template. (B) Docking of the predicted Tax GID structure and GSK-3 β . (C) Close-up view of the putative Tax GID α -helix (green) is bound in the hydrophobic groove of GSK-3 formed by the α -helix (aa. 262 – 273) and the extended loop (aa. 285 – 300), where Axin binds.

To test the theoretical prediction of Tax-GSK-3 β interaction, we constructed point and deletion mutations in GSK-3 β to identify the residues and domain(s) involved in its interaction with Tax. Phe-291 on the extended loop (aa. 285 – 300) of GSK-3 β plays an important role binding the ligands such as LANA (131), Axin GID, and FRAT1 (84) in the hydrophobic groove, as the single-point mutation, F291L, causes a 90% reduction of GSK-3 β binding to Axin and FRAT1 (131). Our docking test results suggest that Phe-291 on the activation loop may also be involved in the Tax-GSK-3 β interaction, therefore we constructed and purified the GSK-3 β F291L mutant for GST pull-down assays. We compared GSK-3 β wt with the F291L single-point mutant for their binding to Tax, however, the F291L mutation did not show reduced binding to Tax (Fig. 2.8). To make more aggressive mutants of GSK-3 β , we deleted the α -helix (aa. 262 – 273, named the Δ helix mutant) and the extended loop (aa. 285 – 300, named the Δ loop mutant) in the hydrophobic groove, respectively (Fig. 2.9). When we expressed both deletion mutants of GSK-3 β in 293T cells, we found that the Δ loop mutant to be a faulty fusion protein that runs higher as shown in our Western blot (Fig. 2.10A, lower panel). This may result from aberrant PCR product overlapping in the deletion mutagenesis PCR, although the sequencing results showed that the DNA sequences of the loop domain were deleted. The Δ loop mutant of GSK-3 β was still tested for binding the Axin GID₃₂₀₋₄₂₉ along with the Δ helix mutant and GSK-3 β wt. The Axin GID₃₂₀₋₄₂₉ is a longer version of the Axin GID, which strongly inhibits GSK-3 β kinase activity through direct interaction with the hydrophobic groove of GSK-3 β (130). Figure 2.10A shows that the Axin GID₃₂₀₋

429 peptide interacted with GSK-3 β wt, but failed to interact with both deletion mutants. This observation was further confirmed by the reciprocal Co-IP results (Fig. 2.10B), which is in agreement with the published report showing that Axin GID interacts with the hydrophobic groove of GSK-3 β (84). To this end, the GSK-3 β Δ helix mutant alone serves as a good negative control for showing no interaction with Axin GID. Because the Δ loop mutant is a faulty fusion protein, we only used the Δ helix mutant of GSK-3 β in our later Co-IP experiments for testing Tax binding. To our surprise, we observed that Tax remained bound to the Δ helix mutant of GSK-3 β (Fig. 2.10 C and D), suggesting that the hydrophobic groove of GSK-3 β may not be the binding interface for Tax.

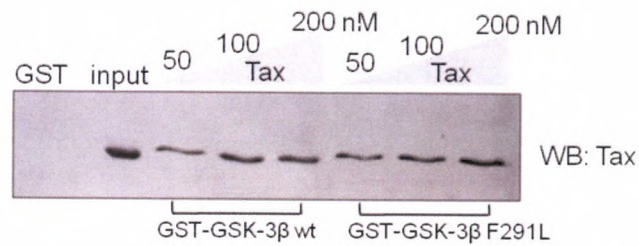


Figure 2.8. Tax remains bound to the GSK-3 β F291L single-point mutant. Wild-type GST-GSK-3 β (wt) and the F291L single-point mutant were compared for Tax binding. Three different amounts of Tax wt were incubated with 50 nM of wt GST-GSK-3 β or F291L mutant as indicated. The GST pull-down assays were analyzed by Western blot (WB) using an anti-Tax antibody. Tax was also tested for binding 50 nM of GST (lane 1). Tax input is shown in lane 2 (2 pmol, 5% of the highest amount of Tax used in the GST pull-down reactions).

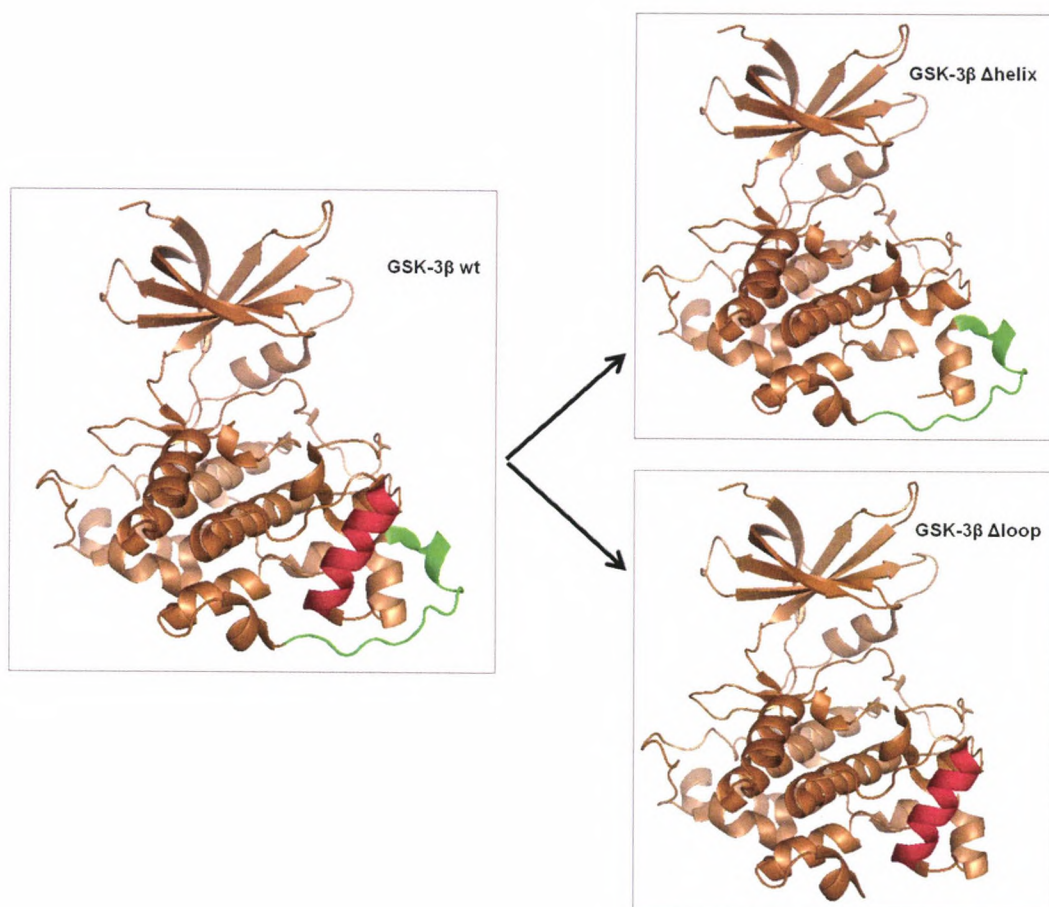


Figure 2.9 Targeted deletion mutagenesis of GSK-3 β binding pocket. The hydrophobic groove of GSK-3 β consists of an α -helix (aa. 262 – 273, red) and an extended loop (aa. 285 – 300, green). The helix and the loop were individually deleted to test their respective roles in Tax binding *in vivo*. The Δ helix mutant of GSK-3 β has the α -helix deleted, and the Δ loop mutant has the extended loop deleted.

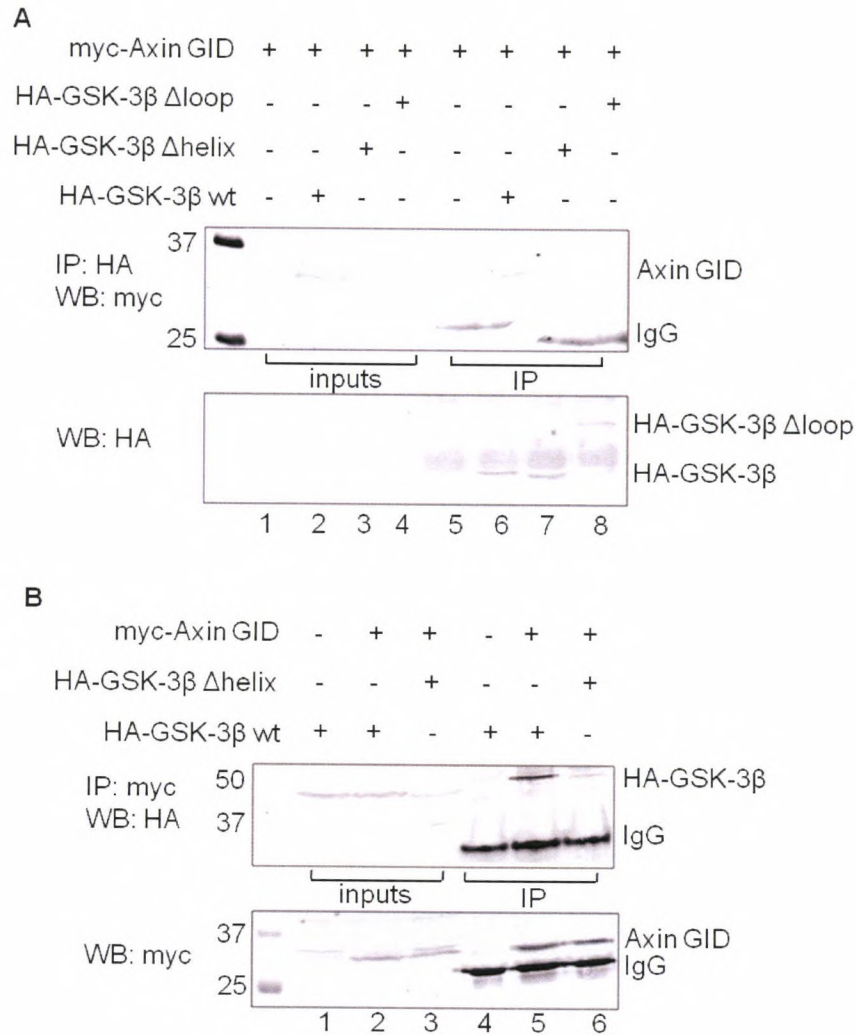


Figure 2.10. Deletion of the GSK-3 β helix has no effect on Tax binding *in vivo*. (A) Control experiment to test whether GSK-3 β deletion mutants abrogate interaction with Axin GID. 293T cells were co-transfected with myc-Axin GID₃₂₀₋₄₂₉ (3 μ g) with or without HA-GSK-3 β wt, Δ helix or Δ loop mutant. The whole cell extracts (WCE) were immunoprecipitated (IP) with an anti-HA antibody, followed by Western blot (WB) analysis with an anti-myc antibody (upper panel). The expression of the transfected HA-GSK-3 β wt, Δ helix, and Δ loop mutants were probed with an anti-HA antibody on the same WB membrane (lower panel). (B) Reciprocal Co-IP experiment of (A) to test whether Axin GID remains bound to the deletion mutants of GSK-3 β .

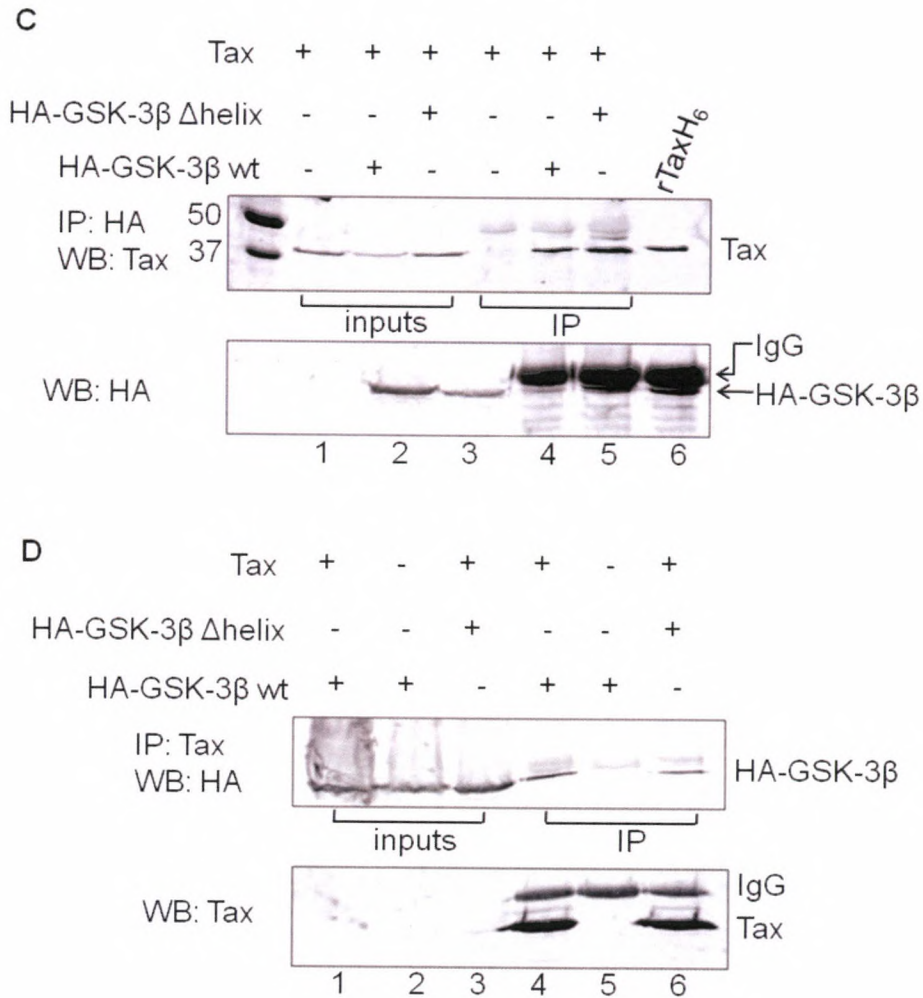


Figure 2.10. (C) 293T cells were co-transfected with 3 μ g of pSG-Tax with or without 3 μ g of HA-GSK-3 β wt or HA-GSK-3 β Δ helix mutant. The WCE were immunoprecipitated with an anti-HA antibody, followed by WB analysis with an anti-Tax antibody (upper panel). The expression of the transfected HA-GSK-3 β wt and Δ helix mutant were probed with an anti-HA antibody on the same WB membrane (lower panel). (D) Reciprocal Co-IP experiment of (C) was performed by using an anti-Tax antibody in the IP from the WCE of transfected 293T cells (upper panel). The expression of transfected pSG-Tax was examined on the same WB membrane by an anti-Tax antibody (lower panel). IgG: immunoglobulin G.

2.4 Discussion

Previous *in vitro* data (reported in Aida Ulloa's M.S. thesis) from the Nyborg laboratory indicated that Tax physically interacts with GSK-3 β , and this interaction results in strong inhibition of GSK-3 β kinase activity towards both primed and non-primed substrates. The data presented here further extended that finding. In this study, we set out to understand the molecular mechanism by which Tax binds and inhibits GSK-3 β . Because Tax structural information is very sparse, we addressed this question by comparing Tax with the well-characterized GSK-3 β interacting proteins: Axin and FRAT1. Both Axin and FRAT1 have been studied for their interaction with GSK-3 β in molecular details, and the peptides derived from their GSK-3 β interacting domains were shown to inhibit GSK-3 β (130, 145). Our analysis of Tax amino acid sequence revealed a putative Tax GID (Tax aa. 185 – 205) that has very notable sequence homology with Axin GID. We used site-directed mutagenesis, rather than deletion mutants, to identify whether the putative Tax GID is involved in the interaction with GSK-3 β , because it is believed that Tax is sensitive to structural change. We observed that only the Tax 5A but none of our single-point Tax mutants diminishes interaction with GSK-3 β . This indicates that the Tax-GSK-3 β interaction may be predominantly hydrophobic, rather than residue-specific interaction. The table 2.1 lists all the Tax mutants that we have characterized. Among all the mutants, the Tax 5A and L194P mutants cannot be expressed in transfected 293T cells. The mutated residues in these two mutants do not give rise to rare codons for human cells (see http://www.genscript.com/cgi-bin/tools/rare_codon_analysis). These two

mutants, however, may have caused Tax protein misfolding, which leads to rapid degradation in cells.

Our biochemical characterization showed that a peptide derived from Tax GID₁₃₈₋₂₀₅ strongly inhibits GSK-3 β *in vitro*. Furthermore, the inhibition potency of Tax GID₁₃₈₋₂₀₅ against GSK-3 β is quite similar to that of full-length Tax (Fig. 2.5C), which suggests that the region aa. 138 – 205 in Tax plays a primary role inhibiting GSK-3 β . As previously reported, both Axin GID and FRATtide peptides inhibit GSK-3 β by binding to the hydrophobic channel on the C-terminal helical domain. However, it is still unclear how binding of the short peptides leads to inhibition of GSK-3 β kinase activity (82, 84, 145). Our Co-IP studies using the GSK-3 β Δ helix deletion mutant indicated that the hydrophobic groove of GSK-3 β is not the binding interface for Tax. This implies that the mechanism of GSK-3 β inhibition by Tax may be different from those used by Axin GID and FRATtide.

In summary, this study extended the initial discovery that Tax inhibits GSK-3 β through direct interaction. Site-directed mutagenesis of Tax revealed that the Tax GID is important for its stable protein-protein interaction with GSK-3 β . Furthermore, we demonstrate that a peptide derived from Tax amino acids 138 – 205 inhibits GSK-3 β kinase activity to the similar degree to Tax does. However, the Tax-binding interface on GSK-3 β is not at the hydrophobic surface channel that both Axin and FRAT1 bind.

Tax mutants	GST pull-down	GSK-3 β kinase assays	Co-IP	Reduced Binding to GSK-3 β
E192A and E193A	+	-	-	-
L194E	+	-	-	-
L194P	+	-	+	-
L195A	+	-	-	-
K197A	+	-	-	-
I198A	+	-	-	-
Tax 3A	+	-	-	+
Tax 5A	+	+	+	+++
F78A	+	-	-	-
S77L, F78A, and R82A	+	-	-	-

Table 2.1. Summary of the characterized Tax mutants. Each Tax mutant was purified and tested for binding GSK-3 β , and selected mutants were characterized by Co-IP and GSK-3 β kinase assays, as indicated.

2.5 Acknowledgements

We thank Drs. Peter Klein and Bert Vogelstein for plasmid constructs and reagents, and the Nyborg lab members for critiques. I thank Dinaida Egan for technical assistance and the purified CREB and GST-KIX proteins. In addition, I appreciate the input and suggestions that I received from my student advisory committee members.

Chapter 3 Supplemental Data

The data in this section include experiments that were conducted but not presented in chapter 2. Some of these data are negative data, which I tried to use for steering my later research in a more positive direction. And although negative, these data are still informative in defining the interaction between Tax and GSK-3 β .

3.1 The Tax 3A mutant (E193A, L194A, and L195A) shows weaker interaction with GSK-3 β .

The search for the identity of Tax residues involved in the Tax-GSK-3 β interaction was started with the construction of single-point mutations within the putative Tax GID region (aa. 185 – 205) in full-length Tax. However, none of the single-point mutations showed diminished interaction with GSK-3 β . Therefore, I selected two additional residues for constructing the Tax 3A mutant. Each mutation carried an alanine substitution at Glu-193, Leu-194, and Leu-195. Our GST pull-down assays with the Tax 3A mutant show that this multi-point mutant weakened its interaction with GSK-3 β (Fig. 3.1). Based on this result, I made the Tax 5A mutant that shows diminished interaction with GSK-3 β .

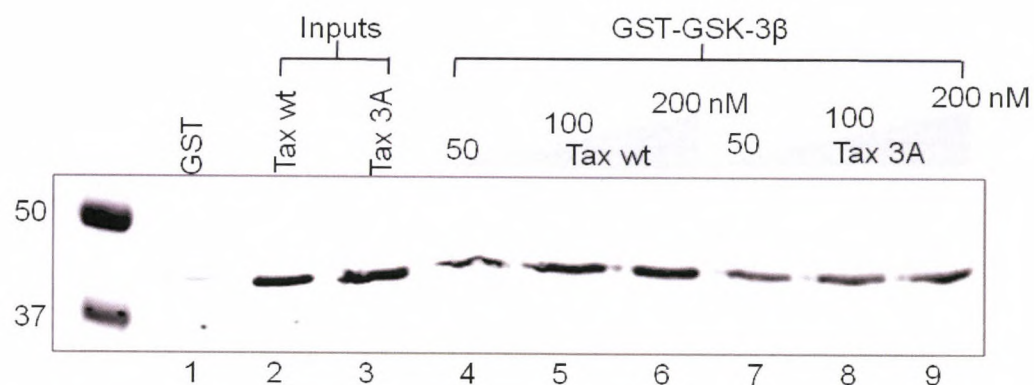


Figure 3.1. The Tax 3A mutant exhibits modestly reduced interaction with GST-GSK-3 β . Wild-type Tax (lanes 4 – 6) and the Tax 3A (lanes 7 – 9) mutant (E193A, L194A, and L195A) were compared for binding GST-GSK-3 β . Amounts of each protein are indicated. GST was also tested for Tax binding (lane 1). The input lanes contain 1 pmol of Tax wt or 3A mutant, which is 2.5% of the highest amount (40 pmol, lane 6 and 9) of Tax used in the GST pull-down assays.

3.2 Tax 5A mutant is defective for quaternary complex formation with CREB/vCRE/KIX.

Having shown that the Tax 5A mutant diminishes its interaction with GSK-3 β , we were interested in examining whether this mutant affects Tax structural competency. To test this possibility, we performed electrophoretic mobility shift assays (EMSAs) using CREB, ³²P-end-labeled viral CRE probe (vCRE), and wild-type Tax or the 5A mutant. CREB binds the vCRE, which is immediately flanked by GC-rich sequences where Tax binds (17). This ternary complex together recruits the KIX domain of CBP to vCRE (25, 26). EMSA has been widely used for studying DNA-binding proteins. We were interested in examining whether the mutated residues in Tax 5A mutant have any adverse effects on complex formation with CREB/vCRE/KIX.

Surprisingly, the Tax 5A mutant was defective for protein complex formation with with CREB/vCRE (Fig. 3.2, compare lanes 7 – 8 and lanes 14 – 15). This may result from the potential impairment of Tax dimerization due to the five mutated residues within the dimerization domain (aa. 127 – 228) (68), as Tax dimerization is required for the efficient ternary complex formation with CREB/vCRE and optimal transactivation (57, 59). The mutated residues may cause local disorder in its dimerization domain and possibly further destabilize the quaternary complex. Moreover, disordered regions in general often lead to difficulties in protein expression and purification (150), which may account for the difficult expression and purification process of Tax 5A mutant and some of my single-point Tax mutant proteins (e.g. Tax L194→P) from bacteria.

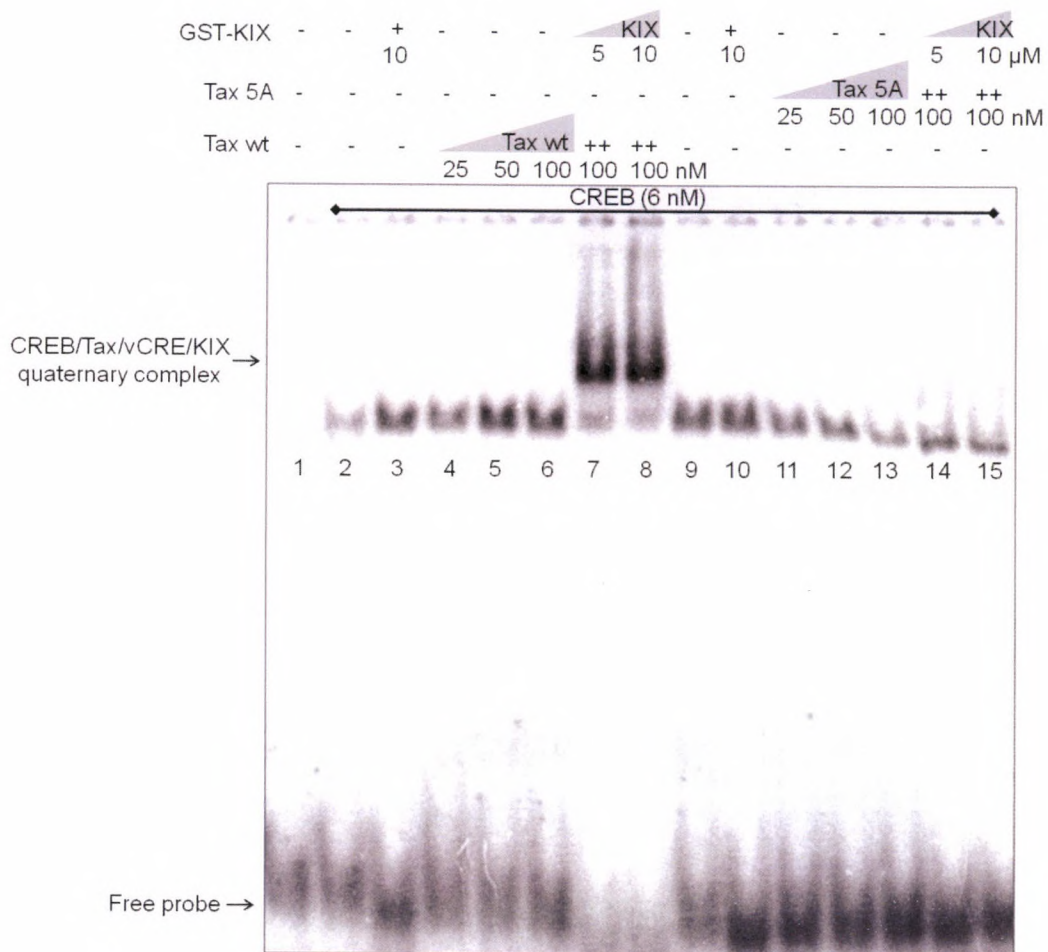


Figure 3.2. Tax 5A is defective for quaternary complex formation with CREB and KIX on HTLV-1 vCRE. EMSAs were performed with (γ - 32 P) end-labeled vCRE probe (0.15 nM), CREB (6 nM) and increasing amounts of Tax (lanes 4 – 6) or Tax 5A (lanes 11 – 13) (25, 50, and 100 nM). GST-KIX-(588 – 683) was added to reactions in two different amounts (5 μ M and 10 μ M), as indicated. Lanes 3 and 10 contain 10 μ M of GST-KIX each. Supershift of the quaternary complex is indicated.

3.3 Tax 5A mutant inhibits GSK-3 β .

An *in vitro* GSK-3 β kinase assay was performed as described above to determine whether the Tax 5A mutant has any inhibitory effects on GSK-3 β . The Tax 5A mutant was first dialyzed in the GSK-3 β kinase buffer along with wild-type Tax (Tax wt). Increasing amounts of each protein were added to the reactions as indicated. Unexpectedly, Tax 5A inhibited GSK-3 β toward pCREB phosphorylation (Fig. 3.3, lanes 12 – 15).

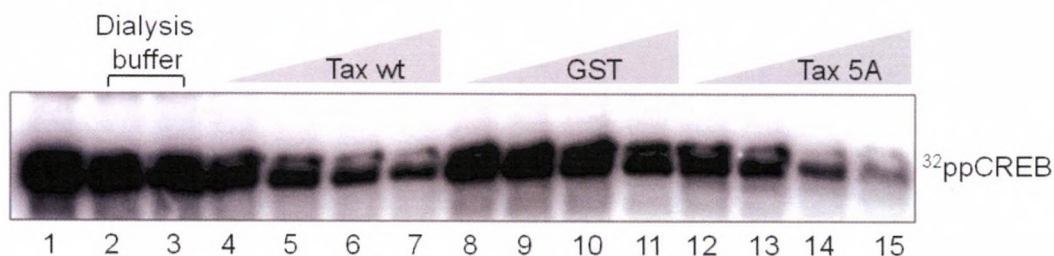


Figure 3.3. Tax 5A mutant inhibits GSK-3 β in a concentration-dependent manner. *In vitro* GSK-3 β kinase assays (20- μ l reaction volume) were performed to compare the activity of Tax 5A mutant and wild-type Tax against GSK-3 β , with GST as a negative control. Four different concentrations (42.5, 85, 170, and 340 nM) of each protein were used in the reactions as indicated. Equal amounts of dialysis buffer (2 μ l) were added to lanes 2 – 3 as negative controls.

3.4 Tax is phosphorylated by GSK-3 β *in vitro*.

We made an unexpected observation in our *in vitro* GSK-3 β kinase assays, which indicated that Tax is phosphorylated by GSK-3 β (Fig. 3.4). In this assay, we incubated Tax and GSK-3 β in the presence of [γ -³²P]-labeled ATP with or without lithium. PKA-primed CREB (pCREB) was used to examine whether GSK-3 β is enzymatically active (lane 2), which can be inhibited by the addition of lithium (lane 3). The phosphorylation of Tax was observed when increasing amounts of either Tax (lanes 5 – 7) or GSK-3 β (lanes 9 – 11) were added. Furthermore, Tax phosphorylation by GSK-3 β can be inhibited by lithium (lanes 8 and 12), and therefore it is not a result of autophosphorylation, as Tax is not a kinase (lane 4). To test whether GSK-3 β phosphorylates protein non-specifically, we used GST-KIX (aa. 588 – 683 of CBP) as a random substrate of GSK-3 β in the kinase assay (lanes 13 – 15). We observed that GSK-3 β did not phosphorylate GST-KIX randomly. Additionally, PKA phosphorylation of CREB (lanes 17 – 18) was used as a standard for quantifying the extent of Tax and pCREB phosphorylation by GSK-3 β , as PKA phosphorylates CREB to almost 100% completion. As indicated in figure 3.4, Tax phosphorylation by GSK-3 β is modest with a maximum phosphorylation efficiency of only 1.3%. Although the phosphorylation efficiency of Tax by GSK-3 β is low compared to pCREB, it is an interesting discovery. We are not sure about the physiological meaning in the context of Tax inhibition of GSK-3 β . The phosphorylation site(s) of Tax by GSK-3 β remains to be characterized.

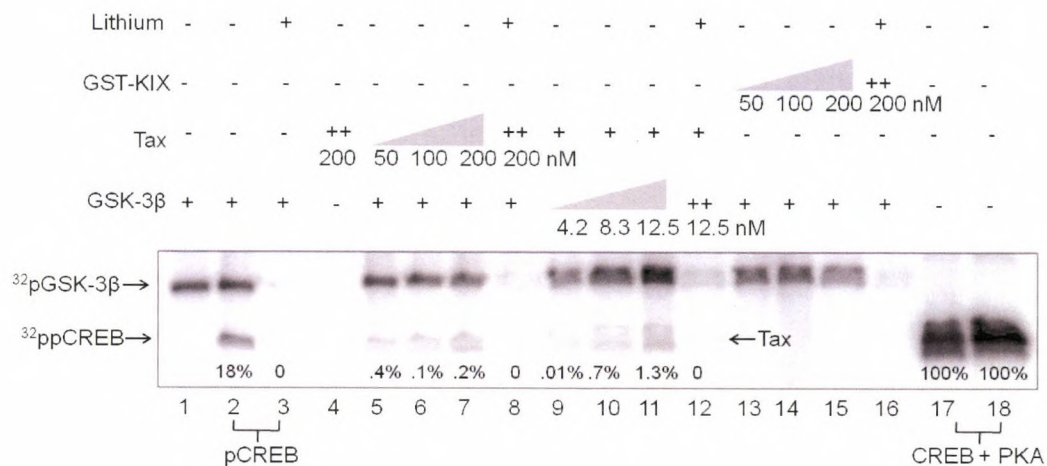


Figure 3.4. Tax is phosphorylated by GSK-3 β *in vitro*. GSK-3 β kinase assays were performed in the presence of Tax or pCREB with or without 100 mM of lithium. Increasing concentrations of Tax (lanes 5 – 7) or GSK-3 β (lanes 9 – 11) were used to titrate Tax phosphorylation while keeping GSK-3 β (4.2 nM) or Tax (50 nM) constant. GST-KIX was used as a random protein to examine whether GSK-3 β phosphorylates substrates non-specifically. PKA phosphorylation of CREB (lanes 17 and 18 contain 5 and 10 nM of CREB, respectively) was used as standards for the quantification of pCREB and Tax phosphorylation by GSK-3 β . PKA-primed CREB of 5 nM was used in lanes 2 and 3 for phosphorylation by GSK-3 β . The percentages of substrates phosphorylation were indicated under each band.

3.5 Tax has little effect on β -catenin/TCF-4 transcriptional activation.

Analysis of the β -catenin activation is an indirect way to study GSK-3 β inactivation *in vivo* (130, 132). We were interested in investigating the effects of Tax-GSK-3 β interaction on the β -catenin pathway. If Tax inhibits GSK-3 β *in vivo*, we would expect to see accumulation of cytoplasmic β -catenin released from the destruction complex (APC/Axin/GSK-3 β / β -catenin) in the Wnt pathway. Stabilized β -catenin binds to TCF-4 to form a transcriptionally active complex (97), which further activates target genes including c-myc (47) and cyclin D1 (48). For this reason, we evaluated the ability of Tax to activate the β -catenin/TCF-4-responsive gene transcription using β -catenin/TCF-4 luciferase reporter plasmids (47) (Fig. 3.5A). The mutant reporter pGL3-OF has three mutated TCF-4 binding sites, rendering β -catenin/TCF-4 unable to activate it. Axin GID was used as a positive control in this assay, which inhibits GSK-3 β and activates the pGL3-OT wild-type reporter as indicated in figure 3.5B, consistent with the published reports (84, 130). However, Tax activation of the pGL3-OT reporter is much lower with a maximum activation of only 3.5-fold. (Fig. 3.5C). To test whether the transfected Tax is fully active, we performed a separate luciferase assay at the same time using the HTLV-1 LTR luciferase reporter (151). Figure 3.5D shows that Tax potently activates the HTLV-1 LTR reporter, indicating that the transiently transfected Tax is active. We were also interested in comparing Tax and Axin GID in parallel. We therefore transfected 293T cells with same amount of each plasmid (Tax or Axin GID) and either wild-type or mutant luciferase reporter plasmids. Consistently, Axin GID activates the wt reporter strongly, but

not the mutant reporter, indicating that the activation of the wild-type reporter is specifically mediated by β -catenin/TCF-4 (Fig. 3.5E). In contrast, Tax has < 2-fold effects on the wild-type reporter activation, which suggests that Tax does not have significant activation effects on the GSK-3 β / β -catenin pathway. Furthermore, it is noteworthy that Tax has similar activation effects on the mutant reporter to the wt reporter, indicating that Tax exerts its modest effects directly on both reporter plasmids, rather than through the β -catenin/TCF-4 pathway.

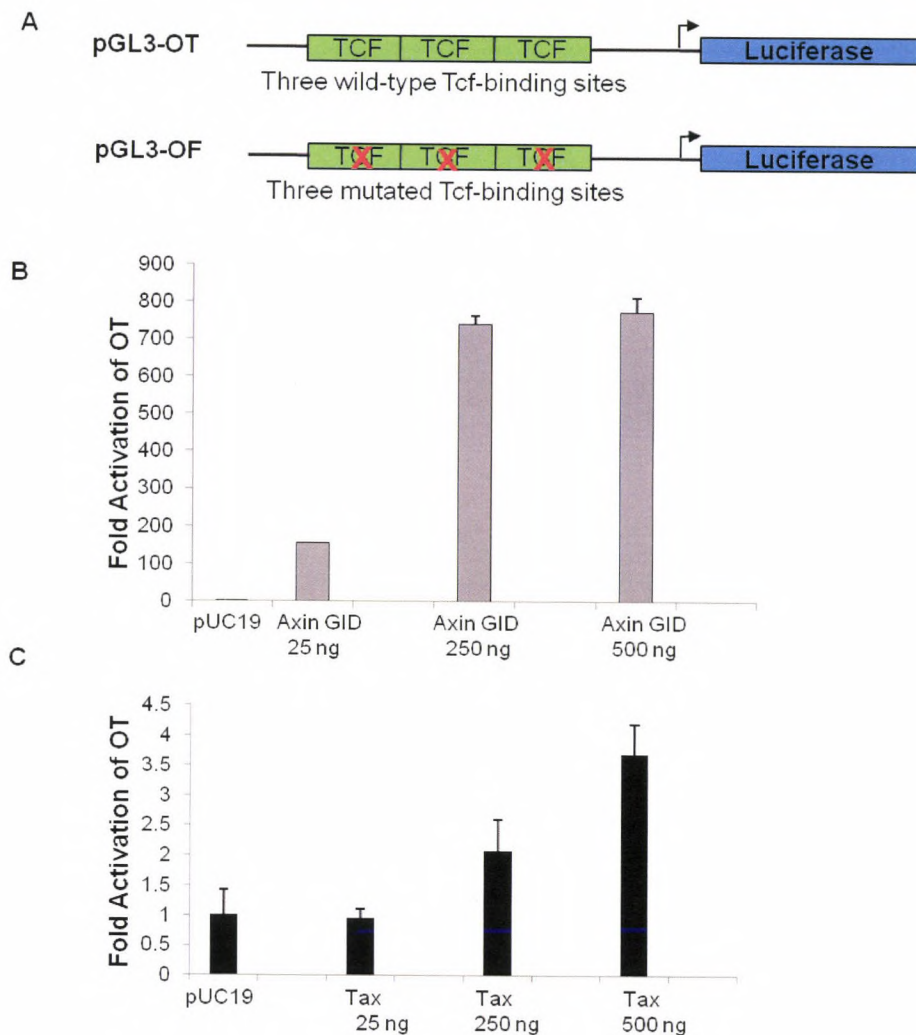


Figure 3.5. Tax has little effects on β -catenin/TCF-4 transcriptional activation. (A) Schematic diagram of the luciferase reporter constructs containing three wild-type (OT) or mutant (OF) TCF-binding sites. (B) Axin GID₃₂₀₋₄₂₉ was used as a positive control for activating the OT reporter. 293T cells were cotransfected with the OT reporter plasmids (100 ng) and Axin GID₃₂₀₋₄₂₉ or the mock vector pUC 19, together with *Renilla* luciferase pRL-TK (10 ng, internal control). Increasing amounts (25 – 500 ng) of Axin GID₃₂₀₋₄₂₉ were used to titrate the activation of the OT reporter. (C) Tax was tested for activating the OT reporter at three different amounts as indicated. Relative fold activation represents luciferase activity normalized to the pUC 19 control.

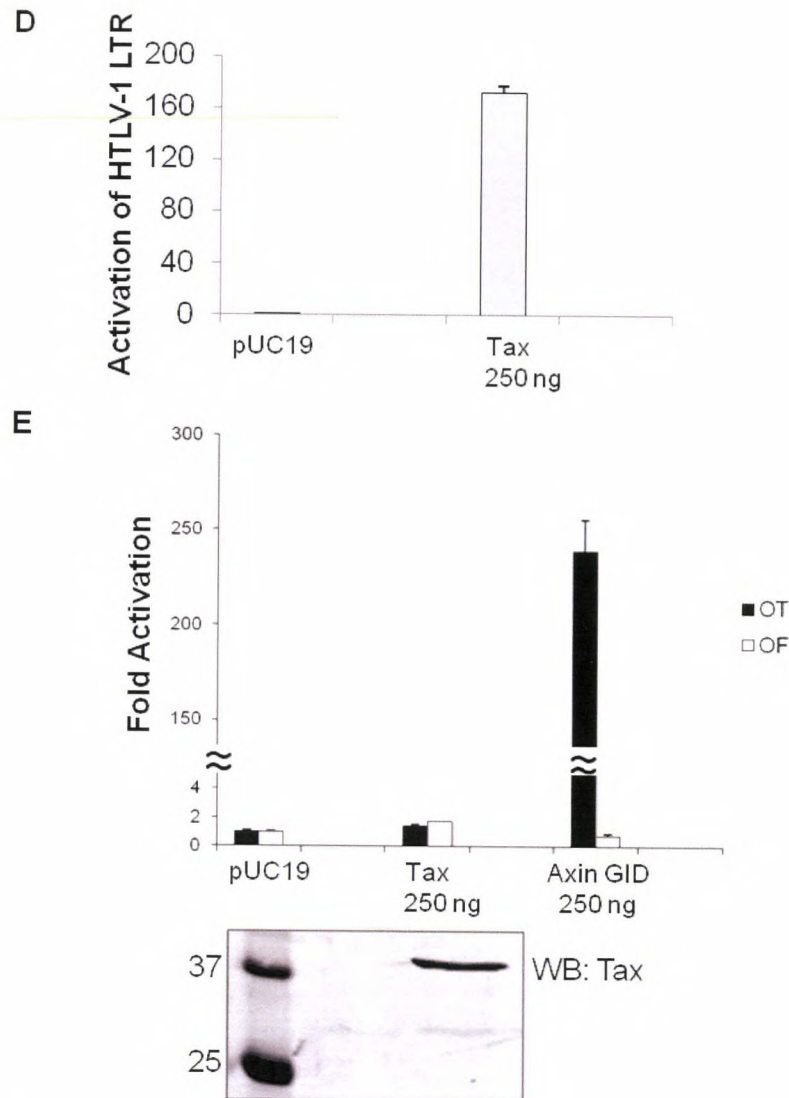


Figure 3.5. (D) Tax is functional for transactivating HTLV-1 LTR. 293T cells were co-transfected with HTLV-1 LTR luciferase reporter (200 ng) and 250 ng of pSG-Tax or pUC19 plasmids. Each transfection was repeated twice. Luciferase activities were assayed 24 hrs after transfection and normalized to pUC19. (E) 293T cells were co-transfected with pGL3-OT or pGL3-OF reporter plasmids and 250 ng of pSG-Tax, pUC19 or Axin GID₃₂₀₋₄₂₉. Transient transfections were performed in duplicate, and each experiment was repeated twice. Relative luciferase activities were assayed 24 hrs after transfection and normalized to pUC19. Error bars denote the standard deviation of the fold activation. Tax expression was probed by Western blot (lower panel) for the corresponding sample analyzed in the luciferase assay.

3.6 Tax has no effect on NFAT transcriptional activation.

Our observation indicates Tax has very minimal activation effects on β -catenin/TCF-4-responsive genes, arguing against the findings reported by Tomita et al (45). We think the effects of Tax inhibition of GSK-3 β may depend on their subcellular localization. As the regulation of β -catenin by GSK-3 β occurs in the cytoplasm, we wanted to switch to the nucleus to study whether Tax inhibits GSK-3 β in the nucleus. NFAT (nuclear factor of activated T-cells) appears to be a good candidate for our purpose, as NFAT is negatively regulated by GSK-3 β . GSK-3 β phosphorylates NFAT and leads to the nuclear export of NFAT, thus inhibiting the expression of NFAT target genes (115, 152), which is reviewed in the reference (113). If Tax inhibits GSK-3 β in the nucleus, we would expect to see elevated activation of NFAT-responsive gene transcription. To this end, we transfected Jurkat T-cells with NFAT luciferase reporter plasmids with other plasmids as indicated in figure 3.6. We first wanted to find a point where HA-GSK-3 β expression inhibits NFAT luciferase reporter activation by 50%. Figure 3.6A shows that 50 ng of HA-GSK-3 β inhibited NFAT by about 50%, however, for some unknown reason; the expression of HA-GSK-3 β seems to have repressing effects on the internal Renilla luciferase (pRL-TK) activity. We had to use a lower amount (20 ng) of HA-GSK-3 β in the following transfection assays.

Once we optimized the transfection conditions for the NFAT assay, we investigated whether Tax had any impact on GSK-3 β repression of NFAT-mediated transcription. We increased the amounts of Tax while keeping GSK-3 β constant in the transfection. However, we observed very minimal effects of Tax

on NFAT activation (Fig. 3.6B). To examine whether the transfected Tax is active, we did a luciferase reporter assay at the same time using HTLV-1 LTR luciferase reporter. Figure 3.6C shows that Tax is functional for transactivating the HTLV-1 LTR luciferase reporter in Jurkat T-cells.

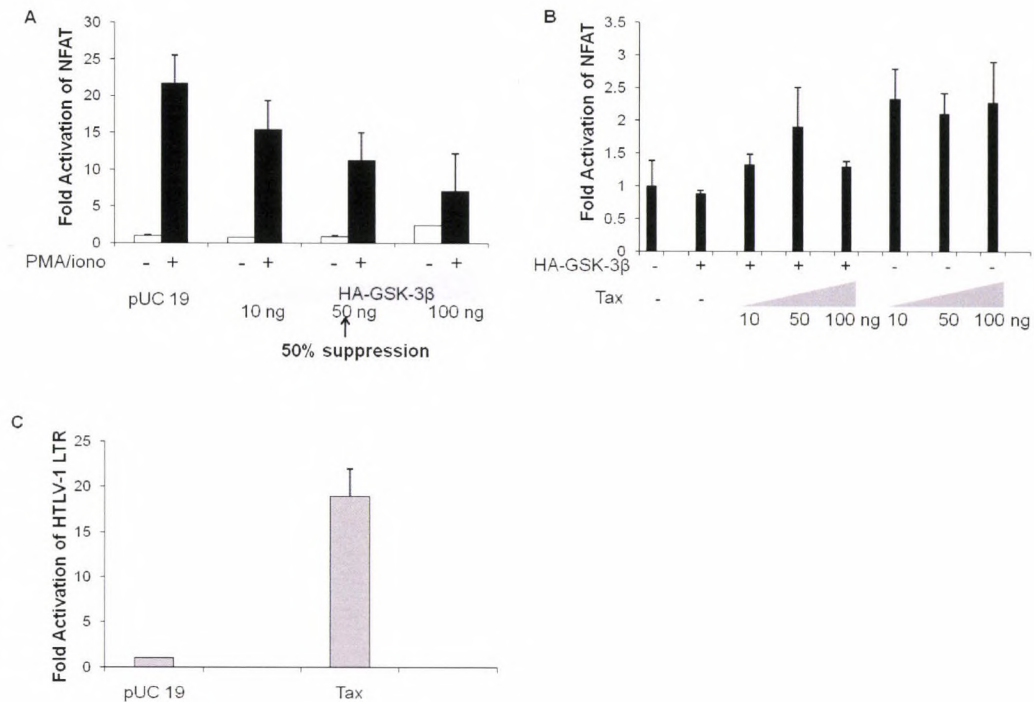


Figure 3.6. Tax has little effects on NFAT activation in Jurkat cells.

(A) GSK-3 β inhibits NFAT activation. HTLV-1-negative Jurkat T-cells were co-transfected with 100 ng of NFAT luciferase reporter plasmids and three different amounts of HA-GSK-3 β as indicated. Cells were transfected for 24 hrs. Six hrs before harvesting, cells were activated with PMA/ionomycin (iono). The luciferase activity of nonactivated cells with pUC 19 transfection was set to 1 arbitrarily. Fifty percent suppression of NFAT luciferase reporter activation by HA-GSK-3 β expression is indicated by an arrow head. (B) Jurkat T-cells were co-transfected as described in (A) with Tax, HA-GSK-3 β (20 ng), or both. Cells were activated by PMA/ionomycin for 6 hrs before harvesting and luciferase activity measurement. (C) Tax is functional for transactivation through the HTLV-1 LTR. Jurkat T-cells were co-transfected with the HTLV-1 LTR luciferase reporter plasmids (100 ng) and pSG-Tax or pUC19 for 24 hrs. Results show average of fold activation \pm standard deviation of three independent experiments.

Chapter 4 Materials and Methods

4.1 Cloning, expression, and purification of recombinant proteins.

The glutathione-S-transferase was made by PCR amplification of the corresponding Tax DNA sequence from the pTaxH₆ plasmid. The PCR products were cloned into the Gateway pDEST 15, with GST tag DNA sequence at the upstream (Invitrogen). The GST-GSK-3 β expression plasmid was constructed as described in Aida Ulloa's thesis. The GST-Tax GID₁₃₈₋₂₀₅ and GST-GSK-3 β expression plasmids were then transformed into *Escherichia coli* BL21(DE3) Codon Plus cells (Stratagene), separately, and induced by 0.2 mM of IPTG for 4 hrs at room temperature. The induced GST-Tax GID₁₃₈₋₂₀₅, wild-type GST-GSK-3 β , and the point mutant GST-GSK-3 β F291L were purified using glutathione agarose chromatography.

C-terminally histidine-tagged Tax (TaxH₆) was expressed from a pTaxH₆ expression plasmid as previously described (71, 153), and purified by nickel-chelate chromatography as described previously (154). The Tax 5A mutant (E193→A, L194→A, L195→, K197→A, and I198→A) was made using the QuickChange site-directed mutagenesis kit (Stratagene) in the pTaxH₆ background (153), followed by bacterial expression and purification by nickel-chelate chromatography.

Two deletion mutants, GSK-3 β Δ helix and GSK-3 β Δ loop, were constructed in the HA-GSK-3 β plasmid using the SLIM (Site-directed, Ligase-independent Mutagenesis) method as previously described (155). Briefly, four primers were designed to delete the α -helix (aa. 262 – 273) or the extended loop (aa. 285 – 300) of GSK-3 β . The primer sequences for deleting the α -helix are as follows. Overhang tail sequences were underlined. F_T (Forward tailed): ATA TTT CCA GGG GAT AGT GGA ACT CCA ACA AGG GAG CAA ATC; F_S (Forward short): GGA ACT CCA ACA AGG GAG CAA ATC; R_T (Reverse tailed): ACT ATC CCC TGG AAA TAT TGG TTG TCC TAG TAA CAG CTC AGC; R_S (Reverse short): TGG TTG TCC TAG TAA CAG CTC AGC. The primers for deleting the extended loop in GSK-3 β include another four set of primer oligos as follows with overhang tail sequences underscore: F_T: 5'-CAA ATC AGA GAA ATG AAC TGG ACT AAG GTC TTC CGA CCC CGA AC-3'; F_S: 5'-TGG ACT AAG GTC TTC CGA CCC CGA AC-3'; R_T: 5'-GTT CAT TTC TCT GAT TTG CTC CCT TGT TGG AGT TCC CAG GAC-3'; and R_S: 5'-CTC CCT TGT TGG AGT TCC CAG GAC-3'. PCR products mixture (25 μ l) was diluted, digested, and hybridized accordingly.

The full-length CREB protein was expressed and purified as previously described (156), which was followed by phosphorylation using the catalytic subunit of protein kinase A at serine-133 for use in the *in vitro* GSK-3 β kinase assays. pCREB was used as a primed substrate in our *in vitro* GSK-3 β kinase. All proteins were dialyzed against TM buffer (50 mM Tris pH 7.9, 100 mM KCl, 12.5 mM MgCl₂, 1 mM EDTA pH 8.0, 20% (vol/vol) glycerol, 0.025% (vol/vol) Tween-20, and 1 mM DTT), aliquoted and stored at -70 °C.

4.2 GST pull-down assays.

GST pull-down experiments were performed as previously described (157). Briefly, all GST pull-down experiments were performed using 20 μ l of glutathione-agarose beads (GST beads) equilibrated in 0.5X Superdex buffer (25 mM HEPES pH7.9, 10 μ M ZnSO₄, 12.5 mM MgCl₂, 150 mM KCl, 20% glycerol [v/v], 0.1% Nonidet P-40, and 1mM EDTA). The purified GST or GST fusion proteins (500 nM) were incubated with the equilibrated glutathione agarose beads for 2 hours at 4 °C with gentle rotation, followed by washing and incubation with the purified TaxH₆ wt or mutant proteins overnight at 4 °C. The pull-down reactions were washed three times by the pull-down buffer, and the bound wild-type TaxH₆ or mutant proteins were resolved on 10 to 12% sodium dodecyl sulfate polyacrylamide gel (SDS-PAGE), transferred to nitrocellulose membrane for subsequent Western blot analysis using an anti-Tax antibody or anti-His antibody.

4.3 Mammalian expression plasmids, cell culture and transient transfection assays.

The Tax expression plasmid, pSG-Tax has been described previously (158). The *Xenopus* myc-tagged Axin GID₃₈₀₋₄₂₉ pCS2 + MT plasmid (130) for expression in mammalian cells was a generous gift from Peter Klein at the University of Pennsylvania. The immortalized human embryo kidney 293T cells and HeLa cells were cultured in Dulbecco's modified Eagle's medium supplemented with 10% fetal bovine serum, 2 mM L-glutamine, and penicillin-streptomycin. Transient-cotransfection assays were performed in 293T and HeLa cells using Eugene 6 reagent, as indicated in figures. Jurkat T-cells were cultured

in Iscove's modified Dulbecco's medium (IMDM) supplemented with 10% fetal bovine serum (FBS), 2 mM L-glutamine and penicillin–streptomycin. Jurkat cells were co-transfected with Lipofectamine reagent (Invitrogen) and a constant amount of DNA as indicated. Where indicated, the transfected Jurkat cells were treated with PMA (20 ng/ml) and ionomycin (2 μ M) for 6 hrs before harvesting.

4.4 Antibodies.

The following antibodies were used in Western blots: anti-CREB (C-21), anti-phospho-Ser133 CREB, anti-HA, anti-GSK-3 β , and anti-His antibodies were all purchased from Santa Cruz Biotechnology. Myc antibody (9E10) was purchased from Sigma. A monoclonal Tax antibody (Hybridoma 168B17-46-92) was obtained from the National Institutes of Health AIDS Research and Reference Reagent Program.

4.5 *In vitro* GSK-3 β kinase assays.

The GSK-3 β kinase was purchased from Cell Signaling Technology. Kinase assays were performed according to the manufacturer's suggested protocol with modification. Briefly, the kinase assays were performed in a 20- μ l reaction containing GSK-3 β kinase buffer (4 mM MOPS, pH 7.2, 2.5 mM β -glycerophosphate, 1 mM EGTA, 0.4 mM EDTA, 4 mM MgCl₂, 0.05 mM DTT, and 40 μ M BSA), GSK-3 β enzyme of 4.15 nM (Cell Signaling, #7436) and 2 μ Ci [γ -³²P]-ATP in the presence or absence of TaxH₆ or GST-TaxGID₁₃₈₋₂₀₅. Recombinant PKA-phosphorylated CREB of 25 nM, unless indicated otherwise, was used as substrates of GSK-3 β . The reactions were incubated at 30 °C for 45 minutes, which were stopped by addition of 4X SDS dye, and heated at 90 °C for

3 – 5 minutes. The reaction was loaded on a 12% SDS-PAGE gel, which was dried for 40 minutes at 80 °C. Substrates phosphorylation by GSK-3 β was visualized by phosphorimager analysis.

4.6 Phosphatase assays.

The purified recombinant GST-Tax GID₁₃₈₋₂₀₅, Tax wt or the 5A mutant proteins of 350 nM were incubated with 25 nM of radiolabeled ³²pSer133-CREB (³²pCREB), cold pCREB, or ³²pSer129-pSer133-CREB (³²ppCREB) in the GSK-3 β kinase buffer with or without phosphatase inhibitors (Sigma P2850). Reactions were performed at 30 °C for 45 minutes, which were stopped by adding 6 μ l of 4X SDS dye to each reaction (20- μ l volume). Samples were heated at 90 °C for 5 minutes, followed by SDS-PAGE analysis. The gel was dried, and the phosphorylation level of pCREB or ppCREB was visualized by phosphorimager analysis.

4.7 Co-immunoprecipitation assays.

293T cells seeded at 2×10^6 per 10-cm dish were transfected using Fugene 6 reagent (Roche) with expression plasmids for Tax (pSG-Tax) or myc-Axin GID₃₈₀₋₄₂₉ and HA-GSK-3 β as indicated in the figure legends. Cells were harvested 48 hours post transfection, resuspended in 400 μ l lysis buffer (50 mM Tris-HCl pH8, 1% NP-40, 100 mM NaCl, and 1 mM MgCl₂) supplemented with protease inhibitors (2 mM benzamidine, 2 μ g/ml leupeptin, 2 μ g aprotinin, and 1 mM PMSF), and lysed on ice for 30 min. Equal amounts of cell lysates were precleared by mixing with proein A/G agarose beads (20 μ l), followed by centrifugation at 2,500 rpm for 5 min. The supernatant was then incubated with

anti-HA polyclonal antibody, anti-Tax antibody, or anti-myc antibody for overnight at 4°C with rotation, followed by incubation with protein A/G-agarose beads (20 µl) for 2 hours at 4°C. Beads were washed three times with ice-cold PBS, resuspended in 1X SDS dye, and boiled prior to SDS-PAGE separation and Western blotting analysis.

4.8 Electrophoretic Mobility Shift Assays (EMSAs).

EMSAs were performed with indicated recombinant proteins as previously described with minor modifications (71). Briefly, purified CREB, Tax wt or the Tax 5A mutant, or GST-KIX (aa. 588 – 683 of CBP) were incubated with ³²P-end-labeled viral CRE (vCRE) DNA probe and 5 ng of poly(dA)·poly(dT) in a 20-µl reaction volume containing 100 mM of imidazole. Binding reactions were incubated on ice for 60 minutes and resolved on 5% nondenaturing polyacrylamide gels (49:1 (w/w), acrylamide:N,N-methylenebisacrylamide) in a running buffer containing 0.04 M Tris-HCl, 0.306 M glycine, pH 8.5, and 0.1% (v/v) Nonidet P-40. Gels were dried and visualized by PhosphorImager (GE Healthcare). The top strand of the DNA probe used in this study is 5'-TTTCAGGCGTTGACGACAACCCCTCA-3' (vCRE sequence underlined), and the bottom strand is 5'-AAT GAGGGGTTGTCGTCAACGCCTGA-3'. The annealed DNA probe has a 2-bp overhang at each end.

4.9 Luciferase reporter assays.

HeLa, 293T or Jurkat cells were transfected with constant amount of DNA (reporter plasmids and pSG-Tax, Axin GID₃₂₀₋₄₂₉ or pUC 19) using Fugene 6 (Roche) or Lipofectamine reagent (Invitrogen) as noted in the figure legends.

After 24 hrs of transfection, the transfected cells were harvested and lysed, and the luciferase activity was measured using a Turner Designs model TD 20-e luminometer. *Renilla* luciferase activity from the herpes simplex virus thymidine kinase promoter (pRL-TK) was used as an internal control to normalize firefly luciferase activities. The pGL3-OT and pGL3-OF reporter plasmids (159) were generous gifts provided by Dr. Bert Vogelstein (The Sidney Kimmel Comprehensive Cancer Center, Johns Hopkins University School of Medicine, Baltimore, MD). pGL3-OT contains three tandem repeats of the wild-type TCF-binding site, and pGL3-OF contains three mutant TCF-binding sequences at the upstream of the c-fos promoter and the luciferase open reading frame. An HTLV-1 LTR luciferase reporter construct (160) was used to examine the activity of transiently transfected Tax. An NF-AT luciferase reporter plasmid (161) was used to study the effects of Tax inhibition of GSK-3 β on NFAT activation in Jurkat cells. The luciferase assay was performed in triplicate or duplicate, as indicated.

Chapter 5 Future Directions

GSK-3 β is such an important multifunctional kinase that is involved in regulating numerous cellular activities, ranging from glycogen metabolism, gene expression, cell cycling and proliferation, microtubule dynamics, and the Wnt signaling pathway (75, 79, 162). Deregulation of GSK-3 β in cells causes many problems for these signaling pathways that GSK-3 β regulates, which has been linked to many types of human cancer, and neurodegenerative diseases (75). Tax inhibition of GSK-3 β may contribute to the leukemogenesis caused by HTLV-1 infection.

It has been reported that Tax inhibits GSK-3 β indirectly by activating the PI3K/Akt pathway (45); however, our studies presented in the second chapter investigated the same problem, but from a different angle – the direct inhibition of GSK-3 β by Tax. We have successfully localized the region in Tax (aa. 138 – 205) that inhibits GSK-3 β . However, the exact mechanism of the inhibition still remains to be elucidated. To further our understanding of the mechanism of Tax-GSK-3 β interaction, we have also tested our hypothesis by performing site-directed mutagenesis (single-point and deletion mutations) in GSK-3 β protein. Our Co-IP studies using two GSK-3 β deletion mutants that have the α -helix (acids 262 – 273) and the extended loop (amino acids 286 – 300) deleted, respectively shows both deletion mutants still retain the capability to interact with Tax, which

suggests that Tax may interact with more than one domains in GSK-3 β or Tax may interact with a different domain other than the hydrophobic groove in GSK-3 β . In future studies, we can perform random mutagenesis on the surface of both Tax and GSK-3 β proteins, followed by pull-down or fluorescence polarization assays. Additionally, NMR-detected mutational scanning could be an alternative option using competition binding experiments, as explained by Baminger and Ludwiczek in their article (163). Crystallography of the Tax-GSK-3 β protein complex would be the best yet most challenging way to gain greater insights into this protein-protein interaction.

As indicated in our Co-IP and GST pull-down results, Tax binds to GSK-3 β both *in vitro* and *in vivo*, which raises the question whether Tax competes with Axin in binding GSK-3 β . As the elevated level of β -catenin protein and GSK-3 β Ser-9 phosphorylation were observed in HTLV-1-infected T-cells and Tax-transfected cells (45), it would be interesting to study whether Tax can dissociate Axin from binding GSK-3 β . The dissociation of Axin from the destruction complex leads to the stabilization and accumulation of β -catenin in cytoplasm. To address this possibility, we can perform three-color single-molecule FRET (Fluorescence/Förster Resonance Energy Transfer) experiments by attaching one of the three fluorophores (e.g., Cyanine5.5, Cyanine3 and Cyanine5) with spectral overlap to each of the proteins, respectively. The application of single-molecule FRET experiments would provide profound information on the intermolecular dynamics for Tax, GSK-3 β and Axin. Alternatively, we can use fluorescence polarization to compare the affinities between Tax and Axin in

binding GSK-3 β by measuring the dissociation constants (K_d). However, before doing this, we still need to see the biological output of Tax-GSK-3 β in cells.

It has come to our attention that Tax can be phosphorylated by GSK-3 β *in vitro*, as shown in our *in vitro* kinase assays (Fig. 3.4), although the phosphorylation efficiency is much lower than pCREB phosphorylation by GSK-3 β . Phosphorylated Tax may function as a substrate of GSK-3 β , which leads to the inhibition of GSK-3 β . To address this possibility and investigate the GSK-3 β phosphorylation site(s) in Tax, we can use mass spectrometry to analyze the phosphorylation of endogenous Tax immunoprecipitated from HTLV-1-infected T-cells (e.g. SLB-1).

Meanwhile, we will also expand the study to the upstream signaling that regulates GSK-3 β , because Tax may target those signaling pathways for deregulation of GSK-3 β . An interesting kinase named aurora kinase A (AURKA) has been very sparsely studied in the HTLV-1 field. This kinase is an interesting candidate for our future studies, because AURKA interacts with GSK-3 β , and the overexpression of AURKA is associated with increased GSK-3 β Ser-9 phosphorylation (87). We may first explore the effect of Tax expression on the activity of AURKA in mammalian cells, followed by studies on the potential interaction between AURKA and GSK-3 β .

The Tax interactome has been summarized by Boxus et al (68) recently. However, the coverage of their review paper on Tax-interacting proteins is limited to those published studies. An important protein kinase the paper is lacking is GSK-3 β , as no previous studies have reported the interaction between Tax and

GSK-3 β . To gain a broader view of Tax-interacting proteins, we can carry out mRNA-display screening from a natural protein library or combinatorial peptide library (164-166). For a review on the mRNA-display technique, see the reference (167).

Finally, to make this project fit better into the laboratory's major research theme, the future direction of this project will have focuses on understanding the impacts of Tax inhibition of GSK-3 β on CREB-regulated HTLV-1 viral gene transcription. CREB is an important transcription factor involved in HTLV-1 viral and cellular genes transcription. Phosphorylation of CREB at Ser-133 is essential for complex formation with the CRE region of promoter and CBP/p300 (26). CREB Ser-133 phosphorylation creates the phosphorylation motif **SXXXS_p** (where **S_p** denotes the phospho-Ser-133 in CREB), for hierarchical phosphorylation by GSK-3 β . However, contradictory results have been reported regarding the effects of the secondary phosphorylation at CREB Ser-129 on its DNA binding activity (109, 168). To investigate the effects of the secondary phosphorylation on CREB DNA binding activity in the context of HTLV-1 viral transcription, we will first do a gel shift assay to compare the DNA binding activity of pCREB (phospho-Ser-133) and ppCREB (phospho-Ser-129, 133). If different DNA binding activity is observed, we can continue to characterize ppCREB by doing *in vitro* transcription assays to further study the difference between the two forms of CREB in recruiting CBP/p300 and transcription initiation.

In summary, the future studies will shed more light on the mechanism of Tax-GSK-3 β interaction and the Tax inhibition of GSK-3 β . More importantly, the

future directions of this project will enable this project to integrate into the general scheme of Tax-induced cell transformation and HTLV-1 pathogenesis.

References

1. Yoshida, M., Discovery of HTLV-1, the first human retrovirus, its unique regulatory mechanisms, and insights into pathogenesis, *Oncogene*, **24**, 5931 (2005).
2. Kamada N, S. M., Miyamoto K, Sanada I, Sadamori N, Fukahara S, Abe S, Shiraishi Y, Abe T, Kaneko Y, Shimoyama M., Chromosome abnormalities in adult T cell leukemia/lymphoma: a karyotype review committee report, *Cancer Res*, **52**, 1481 (1992).
3. Tokudome, S., Tokunaga, O., Shimamoto, Y., Miyamoto, Y., Sumida, I., Kikuchi, M., Takeshita, M., Ikeda, T., Fujiwara, K., and Yoshihara, M., Incidence of adult T-cell leukemia/lymphoma among human T-lymphotropic virus type I carriers in Saga, Japan, *Cancer Res.*, **49**, 226 (1989).
4. Franchini, G., Molecular mechanisms of human T-cell leukemia/lymphotropic virus type I infection, *Blood*, **86**, 3619 (1995).
5. Taylor, J. M., and Nicot, C., HTLV-1 and apoptosis: role in cellular transformation and recent advances in therapeutic approaches, *Apoptosis*, **13**, 733 (2008).
6. Levin, M. C., Lee, S. M., Kalume, F., Morcos, Y., Dohan, F. C., Jr., Hasty, K. A., Callaway, J. C., Zunt, J., Desiderio, D., and Stuart, J. M., Autoimmunity due to molecular mimicry as a cause of neurological disease, *Nat. Med.*, **8**, 509 (2002).
7. Garcia-Vallejo, F., Dominguez, M. C., and Tamayo, O., Autoimmunity and molecular mimicry in tropical spastic paraparesis/human T-lymphotropic virus-associated myelopathy, *Braz J Med Biol Res*, **38**, 241 (2005).
8. Koyanagi, Y., Itoyama, Y., Nakamura, N., Takamatsu, K., Kira, J., Iwamasa, T., Goto, I., and Yamamoto, N., In vivo infection of human T-cell leukemia virus type I in non-T cells, *Virology*, **196**, 25 (1993).
9. Manel, N., Kim, F. J., Kinet, S., Taylor, N., Sitbon, M., and Battini, J. L., The ubiquitous glucose transporter GLUT-1 is a receptor for HTLV, *Cell*, **115**, 449 (2003).
10. Brady, J., K.-T. Jeang, J. Duvall and G. Khoury, Identification of p40^x-responsive regulatory se-quences within the Human T-cell Leukemia Virus Type I long terminal repeat, *J. Virol*, **61**, 2175 (1987).
11. Grassmann, R., Aboud, M., and Jeang, K. T., Molecular mechanisms of cellular transformation by HTLV-I Tax, *Oncogene*, **24**, 5976 (2005).
12. Sun, S. C., and Yamaoka, S., Activation of NF-kappaB by HTLV-I and implications for cell transformation, *Oncogene*, **24**, 5952 (2005).
13. Cann, A. J., Rosenblatt, J. D., Wachsman, W., Shah, N. P., and Chen, I. S., Identification of the gene responsible for human T-cell leukaemia virus transcriptional regulation, *Nature*, **318**, 571 (1985).
14. Chen, I. S., Slamon, D. J., Rosenblatt, J. D., Shah, N. P., Quan, S. G., and Wachsman, W., The x gene is essential for HTLV replication, *Science*, **229**, 54 (1985).
15. Fujisawa, J., Seiki, M., Kiyokawa, T., and Yoshida, M., Functional activation of the long terminal repeat of human T-cell leukemia virus type I by a trans-acting factor, *Proc. Natl. Acad. Sci. USA*, **82**, 2277 (1985).
16. Seiki, M., Inoue, J., Takeda, T., and Yoshida, M., Direct evidence that p40x of human T-cell leukemia virus type I is a trans-acting transcriptional activator, *EMBO J.*, **5**, 561 (1986).

17. Lenzmeier, B. A., Giebler, H. A., and Nyborg, J. K., Human T-cell leukemia virus type 1 Tax requires direct access to DNA for recruitment of CREB binding protein to the viral promoter, *Mol. Cell. Biol.*, **18**, 721 (1998).
18. Yan, J. P., Garrus, J. E., Giebler, H. A., Stargell, L. A., and Nyborg, J. K., Molecular interactions between the coactivator CBP and the human T-cell leukemia virus Tax protein, *J. Mol. Biol.*, **281**, 395 (1998).
19. Fujisawa, J. I., Seiki, M., Sato, M., and Yoshida, M., A transcriptional enhancer sequence of HTLV-1 is responsible for transactivation mediated by p40^x of HTLV-1, *EMBO J*, **5**, 713 (1986).
20. Paskalis, H., B.K. Felber, G.N. Pavlakis, Cis-acting sequences responsible for the transcriptional activation of human T-cell leukemia virus type I constitute a conditional enhancer, *Proc. Natl. Acad. Sci. USA*, **83**, 6558 (1986).
21. Rosen, C. A., Sodroski, J. G., and Haseltine, W. A., Location of *cis*-acting regulatory sequences in the human T-cell leukemia virus type I long terminal repeat, *Proc. Natl. Acad. Sci. USA*, **82**, 6502 (1985).
22. Rosen, C. A., R. Park, J.G. Sodroski, and W.A. Haseltine, Multiple sequence elements are required for regulation of human T-cell leukemia virus gene expression, *Proc. Natl. Acad. Sci. USA*, **84**, 4919 (1987).
23. Shimotohno, K., Takano, M., Teruuchi, T., and Miwa, M., Requirement of multiple copies of a 21-nucleotide sequence in the U3 region of human T-cell leukemia virus type I and type II long terminal repeats for trans-acting activation of transcription, *Proc Natl Acad Sci USA*, **83**, 8112 (1986).
24. Kwok, R. P., Lurance, M. E., Lundblad, J. R., Goldman, P. S., Shih, H., Connor, L. M., Marriott, S. J., and Goodman, R. H., Control of cAMP-regulated enhancers by the viral transactivator Tax through CREB and the co-activator CBP, *Nature*, **380**, 642 (1996).
25. Geiger, T. R., Sharma, N., Kim, Y. M., and Nyborg, J. K., The human T-cell leukemia virus type 1 tax protein confers CBP/p300 recruitment and transcriptional activation properties to phosphorylated CREB, *Mol Cell Biol*, **28**, 1383 (2008).
26. Kim, Y. M., Ramirez, J. A., Mick, J. E., Giebler, H. A., Yan, J. P., and Nyborg, J. K., Molecular characterization of the Tax-containing HTLV-1 enhancer complex reveals a prominent role for CREB phosphorylation in Tax transactivation, *J Biol Chem*, **282**, 18750 (2007).
27. Kornhauser, J. M., Cowan, C. W., Shaywitz, A. J., Dolmetsch, R. E., Griffith, E. C., Hu, L. S., Haddad, C., Xia, Z., and Greenberg, M. E., CREB transcriptional activity in neurons is regulated by multiple, calcium-specific phosphorylation events, *Neuron*, **34**, 221 (2002).
28. Xing, J., Ginty, D. D., and Greenberg, M. E., Coupling of the RAS-MAPK pathway to gene activation by RSK2, a growth factor-regulated CREB kinase, *Science*, **273**, 959 (1996).
29. Matthews, R. P., Guthrie, C. R., Wailes, L. M., Zhao, X., Means, A. R., and McKnight, G. S., Calcium/calmodulin-dependent protein kinase types II and IV differentially regulate CREB-dependent gene expression, *Mol Cell Biol*, **14**, 6107 (1994).
30. Sun, P., Enslen, H., Myung, P. S., and Maurer, R. A., Differential activation of CREB by Ca²⁺/calmodulin-dependent protein kinases type II and type IV involves phosphorylation of a site that negatively regulates activity, *Genes Dev*, **8**, 2527 (1994).

31. Tan, Y., Rouse, J., Zhang, A., Cariati, S., Cohen, P., and Comb, M. J., FGF and stress regulate CREB and ATF-1 via a pathway involving p38 MAP kinase and MAPKAP kinase-2, *EMBO J*, **15**, 4629 (1996).
32. Meyer, C. J., Alenghat, F. J., Rim, P., Fong, J. H., Fabry, B., and Ingber, D. E., Mechanical control of cyclic AMP signalling and gene transcription through integrins, *Nat Cell Biol*, **2**, 666 (2000).
33. Beitner-Johnson, D., Rust, R. T., Hsieh, T. C., and Millhorn, D. E., Hypoxia activates Akt and induces phosphorylation of GSK-3 in PC12 cells, *Cell Signal*, **13**, 23 (2001).
34. Trevisan, R., Daprai, L., Acquasaliente, L., Ciminale, V., Chieco-Bianchi, L., and Saggiaro, D., Relevance of CREB phosphorylation in the anti-apoptotic function of human T-lymphotropic virus type 1 tax protein in serum-deprived murine fibroblasts, *Exp Cell Res*, **299**, 57 (2004).
35. Trevisan, R., Daprai, L., Paloschi, L., Vajente, N., Chieco-Bianchi, L., and Saggiaro, D., Antiapoptotic effect of human T-cell leukemia virus type 1 tax protein correlates with its creb transcriptional activity, *Exp Cell Res*, **312**, 1390 (2006).
36. Grassmann, R., Dengler, C., Muller-Fleckenstein, I., McGuire, K., Dokhelar, M. C., Sodroski, J. G., and Haseltine, W. A., Transformation to continuous growth of primary human T lymphocytes by human T cell leukemia virus type I X-region genes transduced by a herpesvirus saimiri vector, *Proc Natl Acad Sci USA*, **86**, 3551 (1989).
37. Grassmann, R., Berchtold, S., Radant, I., Alt, M., Fleckenstein, B., Sodroski, J. G., Haseltine, W. A., and Ramstedt, U., Role of human T-cell leukemia virus type 1 X region proteins in immortalization of primary human lymphocytes in culture, *J. Virol.*, **66**, 4570 (1992).
38. Ruckes, T., Saul, D., Van Snick, J., Hermine, O., and Grassmann, R., Autocrine antiapoptotic stimulation of cultured adult T-cell leukemia cells by overexpression of the chemokine I-309, *Blood*, **98**, 1150 (2001).
39. Pise-Masison, C. A., Radonovich, M., Mahieux, R., Chatterjee, P., Whiteford, C., Duvall, J., Guillermin, C., Gessain, A., and Brady, J. N., Transcription profile of cells infected with human T-cell leukemia virus type I compared with activated lymphocytes, *Cancer Res*, **62**, 3562 (2002).
40. Gout, I., Dhand, R., Panayotou, G., Fry, M. J., Hiles, I., Otsu, M., and Waterfield, M. D., Expression and characterization of the p85 subunit of the phosphatidylinositol 3-kinase complex and a related p85 beta protein by using the baculovirus expression system, *Biochem J*, **288** (Pt 2), 395 (1992).
41. Liu, Y., Wang, Y., Yamakuchi, M., Masuda, S., Tokioka, T., Yamaoka, S., Maruyama, I., and Kitajima, I., Phosphoinositide-3 kinase-PKB/Akt pathway activation is involved in fibroblast Rat-1 transformation by human T-cell leukemia virus type I tax, *Oncogene*, **20**, 2514 (2001).
42. Peloponese, J. M., Jr., and Jeang, K. T., Role for Akt/protein kinase B and activator protein-1 in cellular proliferation induced by the human T-cell leukemia virus type 1 tax oncoprotein, *J Biol Chem*, **281**, 8927 (2006).
43. Song, G., Ouyang, G., and Bao, S., The activation of Akt/PKB signaling pathway and cell survival, *J Cell Mol Med*, **9**, 59 (2005).
44. Yu, J., Zhang, Y., McIlroy, J., Rordorf-Nikolic, T., Orr, G. A., and Backer, J. M., Regulation of the p85/p110 phosphatidylinositol 3'-kinase: stabilization and inhibition of the p110alpha catalytic subunit by the p85 regulatory subunit, *Mol Cell Biol*, **18**, 1379 (1998).

45. Tomita, M., Kikuchi, A., Akiyama, T., Tanaka, Y., and Mori, N., Human T-cell leukemia virus type 1 tax dysregulates beta-catenin signaling, *J Virol*, **80**, 10497 (2006).
46. Jeong, S. J., Pise-Masison, C. A., Radonovich, M. F., Park, H. U., and Brady, J. N., Activated AKT regulates NF-kappaB activation, p53 inhibition and cell survival in HTLV-1-transformed cells, *Oncogene*, **24**, 6719 (2005).
47. He, T. C., Sparks, A. B., Rago, C., Hermeking, H., Zawel, L., da Costa, L. T., Morin, P. J., Vogelstein, B., and Kinzler, K. W., Identification of c-MYC as a target of the APC pathway, *Science*, **281**, 1509 (1998).
48. Shtutman, M., Zhurinsky, J., Simcha, I., Albanese, C., D'Amico, M., Pestell, R., and Ben-Ze'ev, A., The cyclin D1 gene is a target of the beta-catenin/LEF-1 pathway, *Proc Natl Acad Sci U S A*, **96**, 5522 (1999).
49. Giles, R. H., van Es, J. H., and Clevers, H., Caught up in a Wnt storm: Wnt signaling in cancer, *Biochim Biophys Acta*, **1653**, 1 (2003).
50. Peifer, M., and Polakis, P., Wnt signaling in oncogenesis and embryogenesis--a look outside the nucleus, *Science*, **287**, 1606 (2000).
51. Chung, E. J., Hwang, S. G., Nguyen, P., Lee, S., Kim, J. S., Kim, J. W., Henkart, P. A., Bottaro, D. P., Soon, L., Bonvini, P., Lee, S. J., Karp, J. E., Oh, H. J., Rubin, J. S., and Trepel, J. B., Regulation of leukemic cell adhesion, proliferation, and survival by beta-catenin, *Blood*, **100**, 982 (2002).
52. Smith, M. R., and Greene, W. C., Characterization of a novel nuclear localization signal in the HTLV-I tax transactivator protein, *Virology*, **187**, 316 (1992).
53. Gitlin, S. D., Lindholm, P. F., Marriott, S. J., and Brady, J. N., Transdominant Human T-cell Lymphotropic Virus Type I TAX₇ mutant that fails to localize to the nucleus, *J. Virol.*, **65**, 2612 (1991).
54. Semmes, O. J., and Jeang, K. T., HTLV-I Tax is a zinc-binding protein: role of Zinc in Tax structure and function, *Virology*, **188**, 754 (1992).
55. Goren, I., Semmes, O. J., Jeang, K. T., and Moelling, K., The amino terminus of Tax is required for interaction with the cyclic AMP response element binding protein, *J. Virol.*, **69**, 5806 (1995).
56. Alefantis, T., Jain, P., Ahuja, J., Mostoller, K., and Wigdahl, B., HTLV-1 Tax nucleocytoplasmic shuttling, interaction with the secretory pathway, extracellular signaling, and implications for neurologic disease, *J Biomed Sci*, **12**, 961 (2005).
57. Jin, D. Y., and K.T. Jeang, HTLV-I Tax self-association in optimal trans-activation function, *Nucleic Acids Res.*, **25**, 379 (1997).
58. Jin, D. Y., and Jeang, K. T., Transcriptional activation and self-association in yeast: Protein-protein dimerization as a pleiotropic mechanism of HTLV-I Tax function, *Leukemia*, **11**, 3 (1997).
59. Tie, F., Adya, N., Greene, W. C., and Giam, C. Z., Interaction of the human T-lymphotropic virus type 1 Tax dimer with CREB and the viral 21-base-pair repeat, *J Virol*, **70**, 8368 (1996).
60. Wu, K., Bottazzi, M. E., de la Fuente, C., Deng, L., Gitlin, S. D., Maddukuri, A., Dadgar, S., Li, H., Vertes, A., Pumfery, A., and Kashanchi, F., Protein profile of tax-associated complexes, *J Biol Chem*, **279**, 495 (2004).
61. Kimzey, A. L., and Dynan, W. S., Identification of a human T-cell leukemia virus type I tax peptide in contact with DNA, *J. Biol. Chem.*, **274**, 34226 (1999).
62. Lenzmeier, B. A., Baird, E. E., Dervan, P. B., and Nyborg, J. K., The tax protein-DNA interaction is essential for HTLV-I transactivation in vitro, *J. Mol. Biol.*, **291**, 731 (1999).

63. Fujii, M., Tsuchiya, H., and Seiki, M., HTLV-1 tax has distinct but overlapping domains for transcriptional activation and for enhancer specificity, *Oncogene*, **6**, 2349 (1991).
64. Adaya, N., and Giam, C. Z., Distinct regions in human T-cell lymphotropic virus type I tax mediate interactions with activator protein CREB and basal transcription factors, *J. Virol.*, **69**, 1834 (1995).
65. Semmes, O. J., and Jeang, K. T., Definition of a minimal activation domain in human T-cell leukemia virus type I Tax, *J. Virol.*, **69**, 1827 (1995).
66. Tsuchiya, H., Fujii, M., Tanaka, Y., Tozawa, H., and Seiki, M., Two distinct regions form a functional activation domain of the HTLV-1 trans-activator Tax1, *Oncogene*, **9**, 337 (1994).
67. Harrod, R., Tang, Y., Nicot, C., Lu, H. S., Vassilev, A., Nakatani, Y., and Giam, C. Z., An exposed KID-like domain in human T-cell lymphotropic virus type 1 Tax is responsible for the recruitment of coactivators CBP/p300, *Mol. Cell. Biol.*, **18**, 5052 (1998).
68. Boxus, M., Twizere, J. C., Legros, S., Dewulf, J. F., Kettmann, R., and Willems, L., The HTLV-1 Tax interactome, *Retrovirology*, **5**, 76 (2008).
69. Siu, Y. T., Chin, K. T., Siu, K. L., Yee Wai Choy, E., Jeang, K. T., and Jin, D. Y., TORC1 and TORC2 coactivators are required for tax activation of the human T-cell leukemia virus type 1 long terminal repeats, *J Virol*, **80**, 7052 (2006).
70. Radhakrishnan, I., Perez-Alvarado, G. C., Parker, D., Dyson, H. J., Montminy, M. R., and Wright, P. E., Solution structure of the KIX domain of CBP bound to the transactivation domain of CREB: a model for activator:coactivator interactions, *Cell*, **91**, 741 (1997).
71. Giebler, H. A., Loring, J. E., van Orden, K., Colgin, M. A., Garrus, J. E., Escudero, K. W., Brauweiler, A., and Nyborg, J. K., Anchoring of CREB binding protein to the human T-cell leukemia virus type 1 promoter: a molecular mechanism of Tax transactivation, *Mol Cell Biol*, **17**, 5156 (1997).
72. Ramirez, J. A., and Nyborg, J. K., Molecular characterization of HTLV-1 tax interaction with the KIX domain of CBP/p300, *J Mol Biol*, **372**, 958 (2007).
73. Dean, J., Hashimoto, K., Tsuji, T., Gautier, V., Hall, W. W., and Sheehy, N., Functional interaction of HTLV-1 tax protein with the POZ domain of the transcriptional repressor BCL6, *Oncogene*, **28**, 3723 (2009).
74. Frame, S., and Cohen, P., GSK3 takes centre stage more than 20 years after its discovery, *Biochem J*, **359**, 1 (2001).
75. Grimes, C. A., and Jope, R. S., The multifaceted roles of glycogen synthase kinase 3beta in cellular signaling, *Prog Neurobiol*, **65**, 391 (2001).
76. Woodgett, J. R., Judging a protein by more than its name: GSK-3, *Sci STKE*, **2001**, RE12 (2001).
77. Woodgett, J. R., Physiological roles of glycogen synthase kinase-3: potential as a therapeutic target for diabetes and other disorders, *Curr Drug Targets Immune Endocr Metabol Disord*, **3**, 281 (2003).
78. Eldar-Finkelman, H., Glycogen synthase kinase 3: an emerging therapeutic target, *Trends Mol Med*, **8**, 126 (2002).
79. Doble, B. W., and Woodgett, J. R., GSK-3: tricks of the trade for a multi-tasking kinase, *J Cell Sci*, **116**, 1175 (2003).
80. ter Haar, E., Coll, J. T., Austen, D. A., Hsiao, H. M., Swenson, L., and Jain, J., Structure of GSK3beta reveals a primed phosphorylation mechanism, *Nat Struct Biol*, **8**, 593 (2001).

81. Dajani, R., Fraser, E., Roe, S. M., Young, N., Good, V., Dale, T. C., and Pearl, L. H., Crystal structure of glycogen synthase kinase 3 beta: structural basis for phosphate-primed substrate specificity and autoinhibition, *Cell*, **105**, 721 (2001).
82. Bax, B., Carter, P. S., Lewis, C., Guy, A. R., Bridges, A., Tanner, R., Pettman, G., Mannix, C., Culbert, A. A., Brown, M. J., Smith, D. G., and Reith, A. D., The structure of phosphorylated GSK-3beta complexed with a peptide, FRATtide, that inhibits beta-catenin phosphorylation, *Structure*, **9**, 1143 (2001).
83. Frame, S., Cohen, P., and Biondi, R. M., A common phosphate binding site explains the unique substrate specificity of GSK3 and its inactivation by phosphorylation, *Mol Cell*, **7**, 1321 (2001).
84. Dajani, R., Fraser, E., Roe, S. M., Yeo, M., Good, V. M., Thompson, V., Dale, T. C., and Pearl, L. H., Structural basis for recruitment of glycogen synthase kinase 3beta to the axin-APC scaffold complex, *EMBO J*, **22**, 494 (2003).
85. Stambolic, V., Ruel, L., and Woodgett, J. R., Lithium inhibits glycogen synthase kinase-3 activity and mimics wingless signalling in intact cells, *Curr Biol*, **6**, 1664 (1996).
86. Sutherland, C., Leighton, I. A., and Cohen, P., Inactivation of glycogen synthase kinase-3 beta by phosphorylation: new kinase connections in insulin and growth-factor signalling, *Biochem J*, **296** (Pt 1), 15 (1993).
87. Dar, A. A., Belkhiri, A., and El-Rifai, W., The aurora kinase A regulates GSK-3beta in gastric cancer cells, *Oncogene*, **28**, 866 (2009).
88. Etienne-Manneville, S., and Hall, A., Cdc42 regulates GSK-3beta and adenomatous polyposis coli to control cell polarity, *Nature*, **421**, 753 (2003).
89. Sinha, D., Wang, Z., Ruchalski, K. L., Levine, J. S., Krishnan, S., Lieberthal, W., Schwartz, J. H., and Borkan, S. C., Lithium activates the Wnt and phosphatidylinositol 3-kinase Akt signaling pathways to promote cell survival in the absence of soluble survival factors, *Am J Physiol Renal Physiol*, **288**, F703 (2005).
90. Berridge, M. J., Downes, C. P., and Hanley, M. R., Neural and developmental actions of lithium: a unifying hypothesis, *Cell*, **59**, 411 (1989).
91. Phiel, C. J., Zhang, F., Huang, E. Y., Guenther, M. G., Lazar, M. A., and Klein, P. S., Histone deacetylase is a direct target of valproic acid, a potent anticonvulsant, mood stabilizer, and teratogen, *J Biol Chem*, **276**, 36734 (2001).
92. York, J. D., Ponder, J. W., and Majerus, P. W., Definition of a metal-dependent/Li(+)-inhibited phosphomonoesterase protein family based upon a conserved three-dimensional core structure, *Proc Natl Acad Sci U S A*, **92**, 5149 (1995).
93. Hughes, K., Nikolakaki, E., Plyte, S. E., Totty, N. F., and Woodgett, J. R., Modulation of the glycogen synthase kinase-3 family by tyrosine phosphorylation, *EMBO J*, **12**, 803 (1993).
94. Miller, J. R., The Wnts, *Genome Biol*, **3**, REVIEWS3001 (2002).
95. Miller, J. R., Hocking, A. M., Brown, J. D., and Moon, R. T., Mechanism and function of signal transduction by the Wnt/beta-catenin and Wnt/Ca²⁺ pathways, *Oncogene*, **18**, 7860 (1999).
96. Polakis, P., Wnt signaling and cancer, *Genes Dev*, **14**, 1837 (2000).
97. Barker, N., Morin, P. J., and Clevers, H., The Yin-Yang of TCF/beta-catenin signaling, *Adv Cancer Res*, **77**, 1 (2000).
98. Brantjes, H., Barker, N., van Es, J., and Clevers, H., TCF: Lady Justice casting the final verdict on the outcome of Wnt signalling, *Biol Chem*, **383**, 255 (2002).
99. Novak, A., and Dedhar, S., Signaling through beta-catenin and Lef/Tcf, *Cell Mol Life Sci*, **56**, 523 (1999).

100. Li, L., Yuan, H., Weaver, C. D., Mao, J., Farr, G. H., 3rd, Sussman, D. J., Jonkers, J., Kimelman, D., and Wu, D., Axin and Frat1 interact with dvl and GSK, bridging Dvl to GSK in Wnt-mediated regulation of LEF-1, *EMBO J*, **18**, 4233 (1999).
101. Hsu, W., Zeng, L., and Costantini, F., Identification of a domain of Axin that binds to the serine/threonine protein phosphatase 2A and a self-binding domain, *J Biol Chem*, **274**, 3439 (1999).
102. Cook, D., Fry, M. J., Hughes, K., Sumathipala, R., Woodgett, J. R., and Dale, T. C., Wingless inactivates glycogen synthase kinase-3 via an intracellular signalling pathway which involves a protein kinase C, *EMBO J*, **15**, 4526 (1996).
103. Dale, T. C., Signal transduction by the Wnt family of ligands, *Biochem J*, **329** (Pt 2), 209 (1998).
104. Bullock, B. P., and Habener, J. F., Phosphorylation of the cAMP response element binding protein CREB by cAMP-dependent protein kinase A and glycogen synthase kinase-3 alters DNA-binding affinity, conformation, and increases net charge, *Biochemistry*, **37**, 3795 (1998).
105. Chrivia, J. C., Kwok, R. P., Lamb, N., Hagiwara, M., Montminy, M. R., and Goodman, R. H., Phosphorylated CREB binds specifically to the nuclear protein CBP, *Nature*, **365**, 855 (1993).
106. Kwok, R. P., Lundblad, J. R., Chrivia, J. C., Richards, J. P., Bachinger, H. P., Brennan, R. G., Roberts, S. G., Green, M. R., and Goodman, R. H., Nuclear protein CBP is a coactivator for the transcription factor CREB, *Nature*, **370**, 223 (1994).
107. Parker, D., Ferreri, K., Nakajima, T., LaMorte, V. J., Evans, R., Koerber, S. C., Hoeger, C., and Montminy, M. R., Phosphorylation of CREB at Ser-133 induces complex formation with CREB- binding protein via a direct mechanism, *Mol. Cell. Biol.*, **16**, 694 (1996).
108. Fiol, C. J., Williams, J. S., Chou, C. H., Wang, Q. M., Roach, P. J., and Andrisani, O. M., A secondary phosphorylation of CREB341 at Ser129 is required for the cAMP-mediated control of gene expression. A role for glycogen synthase kinase-3 in the control of gene expression, *J Biol Chem*, **269**, 32187 (1994).
109. Grimes, C. A., and Jope, R. S., CREB DNA binding activity is inhibited by glycogen synthase kinase-3 beta and facilitated by lithium, *J Neurochem*, **78**, 1219 (2001).
110. Liu, C., Li, Y., Semenov, M., Han, C., Baeg, G. H., Tan, Y., Zhang, Z., Lin, X., and He, X., Control of beta-catenin phosphorylation/degradation by a dual-kinase mechanism, *Cell*, **108**, 837 (2002).
111. Amit, S., Hatzubai, A., Birman, Y., Andersen, J. S., Ben-Shushan, E., Mann, M., Ben-Neriah, Y., and Alkalay, I., Axin-mediated CKI phosphorylation of beta-catenin at Ser 45: a molecular switch for the Wnt pathway, *Genes Dev*, **16**, 1066 (2002).
112. Yanagawa, S., Matsuda, Y., Lee, J. S., Matsubayashi, H., Sese, S., Kadowaki, T., and Ishimoto, A., Casein kinase I phosphorylates the Armadillo protein and induces its degradation in Drosophila, *EMBO J*, **21**, 1733 (2002).
113. Macian, F., NFAT proteins: key regulators of T-cell development and function, *Nat Rev Immunol*, **5**, 472 (2005).
114. Chow, C. W., Rincon, M., and Davis, R. J., Requirement for transcription factor NFAT in interleukin-2 expression, *Mol Cell Biol*, **19**, 2300 (1999).
115. Beals, C. R., Sheridan, C. M., Turck, C. W., Gardner, P., and Crabtree, G. R., Nuclear export of NF-ATc enhanced by glycogen synthase kinase-3, *Science*, **275**, 1930 (1997).

116. Diehn, M., Alizadeh, A. A., Rando, O. J., Liu, C. L., Stankunas, K., Botstein, D., Crabtree, G. R., and Brown, P. O., Genomic expression programs and the integration of the CD28 costimulatory signal in T cell activation, *Proc Natl Acad Sci U S A*, **99**, 11796 (2002).
117. Sanchez, C., Diaz-Nido, J., and Avila, J., Phosphorylation of microtubule-associated protein 2 (MAP2) and its relevance for the regulation of the neuronal cytoskeleton function, *Prog Neurobiol*, **61**, 133 (2000).
118. Avila, J., Dominguez, J., and Diaz-Nido, J., Regulation of microtubule dynamics by microtubule-associated protein expression and phosphorylation during neuronal development, *Int J Dev Biol*, **38**, 13 (1994).
119. Mandell, J. W., and Banker, G. A., Microtubule-associated proteins, phosphorylation gradients, and the establishment of neuronal polarity, *Perspect Dev Neurobiol*, **4**, 125 (1996).
120. Tokuda, M., and Hatase, O., Regulation of neuronal plasticity in the central nervous system by phosphorylation and dephosphorylation, *Mol Neurobiol*, **17**, 137 (1998).
121. Gundersen, G. G., and Cook, T. A., Microtubules and signal transduction, *Curr Opin Cell Biol*, **11**, 81 (1999).
122. Hong, M., Chen, D. C., Klein, P. S., and Lee, V. M., Lithium reduces tau phosphorylation by inhibition of glycogen synthase kinase-3, *J Biol Chem*, **272**, 25326 (1997).
123. Hanger, D. P., Hughes, K., Woodgett, J. R., Brion, J. P., and Anderton, B. H., Glycogen synthase kinase-3 induces Alzheimer's disease-like phosphorylation of tau: generation of paired helical filament epitopes and neuronal localisation of the kinase, *Neurosci Lett*, **147**, 58 (1992).
124. Mandelkow, E. M., Drewes, G., Biernat, J., Gustke, N., Van Lint, J., Vandenheede, J. R., and Mandelkow, E., Glycogen synthase kinase-3 and the Alzheimer-like state of microtubule-associated protein tau, *FEBS Lett*, **314**, 315 (1992).
125. Johnson, G. V., and Hartigan, J. A., Tau protein in normal and Alzheimer's disease brain: an update, *J Alzheimers Dis*, **1**, 329 (1999).
126. Wille, H., Mandelkow, E. M., Dingus, J., Vallee, R. B., Binder, L. I., and Mandelkow, E., Domain structure and antiparallel dimers of microtubule-associated protein 2 (MAP2), *J Struct Biol*, **108**, 49 (1992).
127. Ainsztein, A. M., and Purich, D. L., Stimulation of tubulin polymerization by MAP-2. Control by protein kinase C-mediated phosphorylation at specific sites in the microtubule-binding region, *J Biol Chem*, **269**, 28465 (1994).
128. Berling, B., Wille, H., Roll, B., Mandelkow, E. M., Garner, C., and Mandelkow, E., Phosphorylation of microtubule-associated proteins MAP2a,b and MAP2c at Ser136 by proline-directed kinases in vivo and in vitro, *Eur J Cell Biol*, **64**, 120 (1994).
129. Sanchez, C., Tompa, P., Szucs, K., Friedrich, P., and Avila, J., Phosphorylation and dephosphorylation in the proline-rich C-terminal domain of microtubule-associated protein 2, *Eur J Biochem*, **241**, 765 (1996).
130. Zhang, F., Phiel, C. J., Spece, L., Gurvich, N., and Klein, P. S., Inhibitory phosphorylation of glycogen synthase kinase-3 (GSK-3) in response to lithium. Evidence for autoregulation of GSK-3, *J Biol Chem*, **278**, 33067 (2003).
131. Fujimuro, M., Liu, J., Zhu, J., Yokosawa, H., and Hayward, S. D., Regulation of the interaction between glycogen synthase kinase 3 and the Kaposi's sarcoma-associated herpesvirus latency-associated nuclear antigen, *J Virol*, **79**, 10429 (2005).

132. Fujimuro, M., Wu, F. Y., ApRhys, C., Kajumbula, H., Young, D. B., Hayward, G. S., and Hayward, S. D., A novel viral mechanism for dysregulation of beta-catenin in Kaposi's sarcoma-associated herpesvirus latency, *Nat Med*, 9, 300 (2003).
133. Hagen, T., Characterization of the interaction between latency-associated nuclear antigen and glycogen synthase kinase 3beta, *J Virol*, 83, 6312 (2009).
134. Thomas, G. M., Frame, S., Goedert, M., Nathke, I., Polakis, P., and Cohen, P., A GSK3-binding peptide from FRAT1 selectively inhibits the GSK3-catalysed phosphorylation of axin and beta-catenin, *FEBS Lett*, 458, 247 (1999).
135. Chou, H. Y., Howng, S. L., Cheng, T. S., Hsiao, Y. L., Lieu, A. S., Loh, J. K., Hwang, S. L., Lin, C. C., Hsu, C. M., Wang, C., Lee, C. I., Lu, P. J., Chou, C. K., Huang, C. Y., and Hong, Y. R., GSKIP is homologous to the Axin GSK3beta interaction domain and functions as a negative regulator of GSK3beta, *Biochemistry*, 45, 11379 (2006).
136. Matsuoka, M., Human T-cell leukemia virus type 1 (HTLV-1) infection and the onset of adult T-cell leukemia (ATL), *Retrovirology*, 2, 2 (2005).
137. Giam, C. Z., and Xu, Y. L., HTLV-I Tax Gene Product Activates Transcription via Pre-existing Cellular Factors and cAMP Responsive Element, *J. Biol. Chem.*, 264, 15236 (1989).
138. Tsuchiya, H., Fujii, M., Niki, T., Tokuhara, M., Matsui, M., and Seiki, M., Human T-cell leukemia virus type 1 Tax activates transcription of the human fra-1 gene through multiple cis elements responsive to transmembrane signals, *J Virol*, 67, 7001 (1993).
139. Hall, W. W., and Fujii, M., Deregulation of cell-signaling pathways in HTLV-1 infection, *Oncogene*, 24, 5965 (2005).
140. Wang, Z., Smith, K. S., Murphy, M., Piloto, O., Somervaille, T. C., and Cleary, M. L., Glycogen synthase kinase 3 in MLL leukaemia maintenance and targeted therapy, *Nature*, 455, 1205 (2008).
141. Willert, K., Shibamoto, S., and Nusse, R., Wnt-induced dephosphorylation of axin releases beta-catenin from the axin complex, *Genes Dev*, 13, 1768 (1999).
142. Ikeda, S., Kishida, S., Yamamoto, H., Murai, H., Koyama, S., and Kikuchi, A., Axin, a negative regulator of the Wnt signaling pathway, forms a complex with GSK-3beta and beta-catenin and promotes GSK-3beta-dependent phosphorylation of beta-catenin, *EMBO J*, 17, 1371 (1998).
143. Gould, T. D., Zarate, C. A., and Manji, H. K., Glycogen synthase kinase-3: a target for novel bipolar disorder treatments, *J Clin Psychiatry*, 65, 10 (2004).
144. Williams, R., Ryves, W. J., Dalton, E. C., Eickholt, B., Shaltiel, G., Agam, G., and Harwood, A. J., A molecular cell biology of lithium, *Biochem Soc Trans*, 32, 799 (2004).
145. Hedgepeth, C. M., Deardorff, M. A., Rankin, K., and Klein, P. S., Regulation of glycogen synthase kinase 3beta and downstream Wnt signaling by axin, *Mol Cell Biol*, 19, 7147 (1999).
146. Baker, D., and Sali, A., Protein structure prediction and structural genomics, *Science*, 294, 93 (2001).
147. Guex, N., and Peitsch, M. C., SWISS-MODEL and the Swiss-PdbViewer: an environment for comparative protein modeling, *Electrophoresis*, 18, 2714 (1997).
148. Schwede, T., Kopp, J., Guex, N., and Peitsch, M. C., SWISS-MODEL: An automated protein homology-modeling server, *Nucleic Acids Res*, 31, 3381 (2003).

149. Arnold, K., Bordoli, L., Kopp, J., and Schwede, T., The SWISS-MODEL workspace: a web-based environment for protein structure homology modelling, *Bioinformatics*, **22**, 195 (2006).
150. Linding, R., Jensen, L. J., Diella, F., Bork, P., Gibson, T. J., and Russell, R. B., Protein disorder prediction: implications for structural proteomics, *Structure*, **11**, 1453 (2003).
151. Okada, M., and Jeang, K. T., Differential requirements for activation of integrated and transiently transfected human T-cell leukemia virus type 1 long terminal repeat, *J. Virol.*, **76**, 12564 (2002).
152. Ohteki, T., Parsons, M., Zakarian, A., Jones, R. G., Nguyen, L. T., Woodgett, J. R., and Ohashi, P. S., Negative regulation of T cell proliferation and interleukin 2 production by the serine threonine kinase GSK-3, *J Exp Med*, **192**, 99 (2000).
153. Zhao, L. J., and Giam, C. Z., Interaction of the human T-cell lymphotropic virus type I (HTLV-I) transcriptional activator Tax with cellular factors that bind specifically to the 21-base-pair repeats in the HTLV-I enhancer, *Proc Natl Acad Sci U S A*, **88**, 11445 (1991).
154. Armstrong, A., Franklin, A., Uittenbogaard, M., Giebler, H., and Nyborg, J., Pleiotropic effect of the Human T-cell Leukemia Virus Tax protein on the DNA binding activity of eucary-otic transcription factors, *Proc Natl Acad Sci USA*, **90**, 7303 (1993).
155. Chiu, J., March, P. E., Lee, R., and Tillett, D., Site-directed, Ligase-Independent Mutagenesis (SLIM): a single-tube methodology approaching 100% efficiency in 4 h, *Nucleic Acids Res*, **32**, e174 (2004).
156. Franklin, A. A., Kubik, M. F., Uittenbogaard, M. N., Brauweiler, A., Utaisinchaoen, P., Matthews, M. A., Dynan, W. S., Hoeffler, J. P., and Nyborg, J. K., Transactivation by the human T-cell leukemia virus Tax protein is mediated through enhanced binding of activating transcription factor-2 (ATF-2) ATF-2 response and cAMP element-binding protein (CREB), *J Biol Chem*, **268**, 21225 (1993).
157. Scoggin, K. E., Ulloa, A., and Nyborg, J. K., The oncoprotein Tax binds the SRC-1-interacting domain of CBP/p300 to mediate transcriptional activation, *Mol Cell Biol*, **21**, 5520 (2001).
158. Rousset, R., Fabre, S., Desbois, C., Bantignies, F., and Jalinot, P., The C-terminus of the HTLV-1 Tax oncoprotein mediates interaction with the PDZ domain of cellular proteins, *Oncogene*, **16**, 643 (1998).
159. Shih, I. M., Yu, J., He, T. C., Vogelstein, B., and Kinzler, K. W., The beta-catenin binding domain of adenomatous polyposis coli is sufficient for tumor suppression, *Cancer Res*, **60**, 1671 (2000).
160. Kibler, K. V., and Jeang, K. T., CREB/ATF-dependent repression of cyclin a by human T-cell leukemia virus type 1 Tax protein, *J Virol*, **75**, 2161 (2001).
161. Kim, L. J., Seto, A. G., Nguyen, T. N., and Goodrich, J. A., Human Taf(II)130 is a coactivator for NFATp, *Mol Cell Biol*, **21**, 3503 (2001).
162. Patel, S., Doble, B., and Woodgett, J. R., Glycogen synthase kinase-3 in insulin and Wnt signalling: a double-edged sword?, *Biochem Soc Trans*, **32**, 803 (2004).
163. Baminger, B., Ludwiczek, M. L., Kontaxis, G., Knapp, S., and Konrat, R., Protein-protein interaction site mapping using NMR-detected mutational scanning, *J Biomol NMR*, **38**, 133 (2007).
164. Roberts, R. W., and Szostak, J. W., RNA-peptide fusions for the in vitro selection of peptides and proteins, *Proc Natl Acad Sci U S A*, **94**, 12297 (1997).

165. Nemoto, N., Miyamoto-Sato, E., Husimi, Y., and Yanagawa, H., In vitro virus: bonding of mRNA bearing puromycin at the 3'-terminal end to the C-terminal end of its encoded protein on the ribosome in vitro, *FEBS Lett*, 414, 405 (1997).
166. Liu, R., Barrick, J. E., Szostak, J. W., and Roberts, R. W., Optimized synthesis of RNA-protein fusions for in vitro protein selection, *Methods Enzymol*, 318, 268 (2000).
167. Valencia, C. A., Cotten, S. W., Dong, B., and Liu, R., mRNA-display-based selections for proteins with desired functions: a protease-substrate case study, *Biotechnol Prog*, 24, 561 (2008).
168. Salas, T. R., Reddy, S. A., Clifford, J. L., Davis, R. J., Kikuchi, A., Lippman, S. M., and Menter, D. G., Alleviating the suppression of glycogen synthase kinase-3 β by Akt leads to the phosphorylation of cAMP-response element-binding protein and its transactivation in intact cell nuclei, *J Biol Chem*, 278, 41338 (2003).